

# Phase-field dislocation dynamics modeling of multi- component alloys

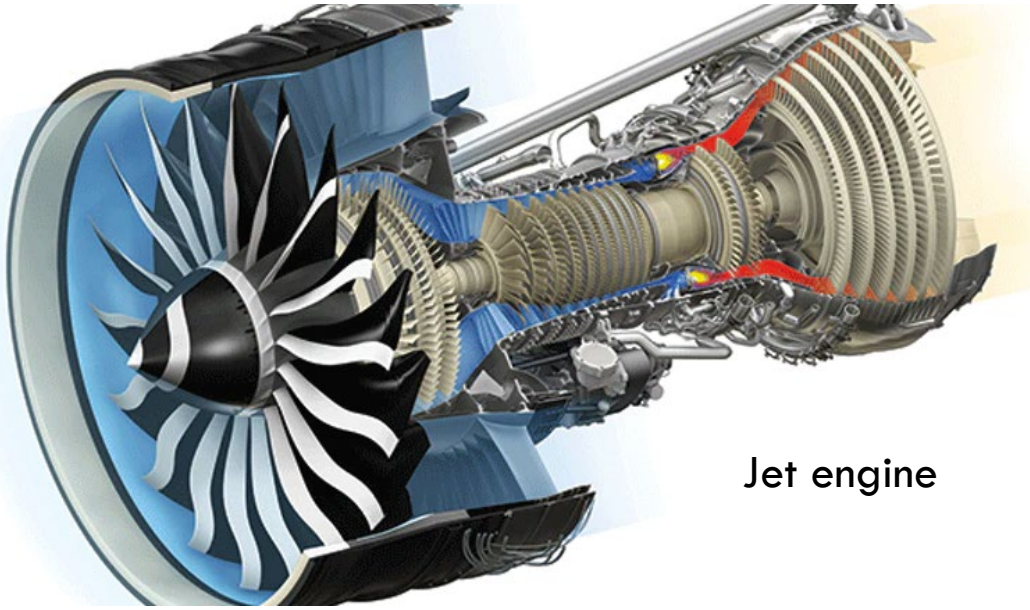


Lauren Fey  
SSGF Program Review  
June 29<sup>th</sup>, 2023

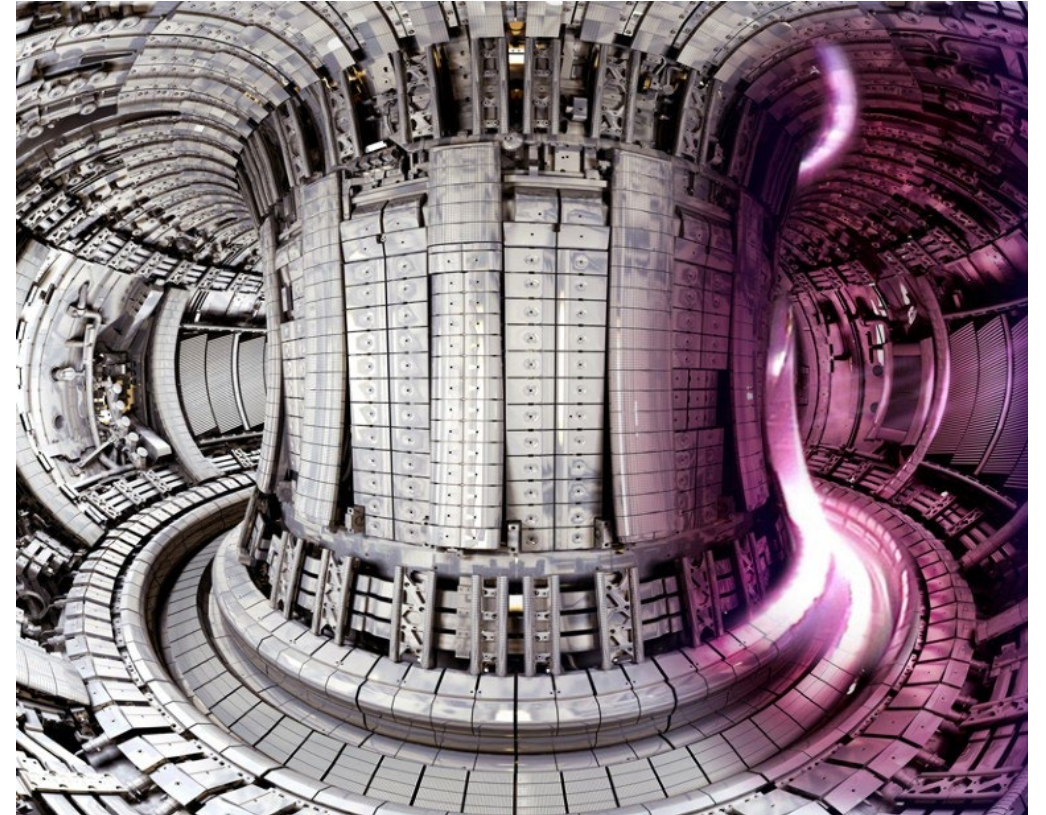


**UC SANTA BARBARA**

# Next-generation materials for extreme environments



Jet engine



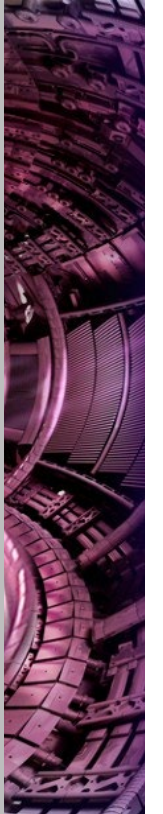
Fusion reactor

# Next-generation materials for extreme environments



**Periodic Table of the Elements**

1 1A 1A																	18 VIIIA 8A
1 H Hydrogen 1.008																	2 He Helium 4.003
3 Li Lithium 6.941	4 Be Beryllium 9.012											5 B Boron 10.811	6 C Carbon 12.011	7 N Nitrogen 14.007	8 O Oxygen 15.999	9 F Fluorine 18.998	10 Ne Neon 20.180
11 Na Sodium 22.99	12 Mg Magnesium 24.305	3 IIIB 3B	4 IVB 4B	5 VB 5B	6 VIB 6B	7 VIIB 7B	8 VIII 8	9 VIII 8	10 VIII 8	11 IB 1B	12 IIB 2B	13 IIIA 3A	14 IVA 4A	15 VA 5A	16 VIA 6A	17 VIIA 7A	18 Ar Argon 39.948
19 K Potassium 39.098	20 Ca Calcium 40.078	21 Sc Scandium 44.956	22 Ti Titanium 47.867	23 V Vanadium 50.942	24 Cr Chromium 51.996	25 Mn Manganese 54.938	26 Fe Iron 55.845	27 Co Cobalt 58.933	28 Ni Nickel 58.693	29 Cu Copper 63.546	30 Zn Zinc 65.38	31 Ga Gallium 69.723	32 Ge Germanium 72.631	33 As Arsenic 74.922	34 Se Selenium 78.971	35 Br Bromine 79.904	36 Kr Krypton 83.799
37 Rb Rubidium 85.468	38 Sr Strontium 87.62	39 Y Yttrium 88.906	40 Zr Zirconium 91.224	41 Nb Niobium 92.906	42 Mo Molybdenum 95.95	43 Tc Technetium 98.907	44 Ru Ruthenium 101.07	45 Rh Rhodium 102.906	46 Pd Palladium 106.42	47 Ag Silver 107.868	48 Cd Cadmium 112.414	49 In Indium 114.818	50 Sn Tin 118.711	51 Sb Antimony 121.760	52 Te Tellurium 127.6	53 I Iodine 126.904	54 Xe Xenon 131.294
55 Cs Cesium 132.905	56 Ba Barium 137.328	57-71 Lanthanide Series	72 Hf Hafnium 178.49	73 Ta Tantalum 180.948	74 W Tungsten 183.84	75 Re Rhenium 186.207	76 Os Osmium 190.23	77 Ir Iridium 192.217	78 Pt Platinum 195.085	79 Au Gold 196.967	80 Hg Mercury 200.592	81 Tl Thallium 204.383	82 Pb Lead 207.2	83 Bi Bismuth 208.980	84 Po Polonium [209]	85 At Astatine [210]	86 Rn Radon 222.018
87 Fr Francium 223.020	88 Ra Radium 226.025	89-103 Actinide Series	104 Rf Rutherfordium [261]	105 Db Dubnium [262]	106 Sg Seaborgium [266]	107 Bh Bohrium [264]	108 Hs Hassium [269]	109 Mt Meitnerium [278]	110 Ds Darmstadtium [281]	111 Rg Roentgenium [280]	112 Cn Copernicium [285]	113 Nh Nihonium [286]	114 Fl Flerovium [289]	115 Mc Moscovium [288]	116 Lv Livermorium [293]	117 Ts Tennessine [294]	118 Og Oganesson [294]
			57 La Lanthanum 138.905	58 Ce Cerium 140.116	59 Pr Praseodymium 140.908	60 Nd Neodymium 144.243	61 Pm Promethium 144.913	62 Sm Samarium 150.36	63 Eu Europium 151.964	64 Gd Gadolinium 157.25	65 Tb Terbium 158.925	66 Dy Dysprosium 162.500	67 Ho Holmium 164.930	68 Er Erbium 167.259	69 Tm Thulium 168.934	70 Yb Ytterbium 173.055	71 Lu Lutetium 174.967
			89 Ac Actinium 227.028	90 Th Thorium 232.038	91 Pa Protactinium 231.036	92 U Uranium 238.029	93 Np Neptunium 237.048	94 Pu Plutonium 244.064	95 Am Americium 243.061	96 Cm Curium 247.070	97 Bk Berkelium 247.070	98 Cf Californium 251.080	99 Es Einsteinium [254]	100 Fm Fermium 257.095	101 Md Mendelevium 258.1	102 No Nobelium 259.101	103 Lr Lawrencium [262]
			Alkali Metal	Alkaline Earth	Transition Metal	Basic Metal	Semimetal	Nonmetal	Halogen	Noble Gas	Lanthanide	Actinide					



# This talk

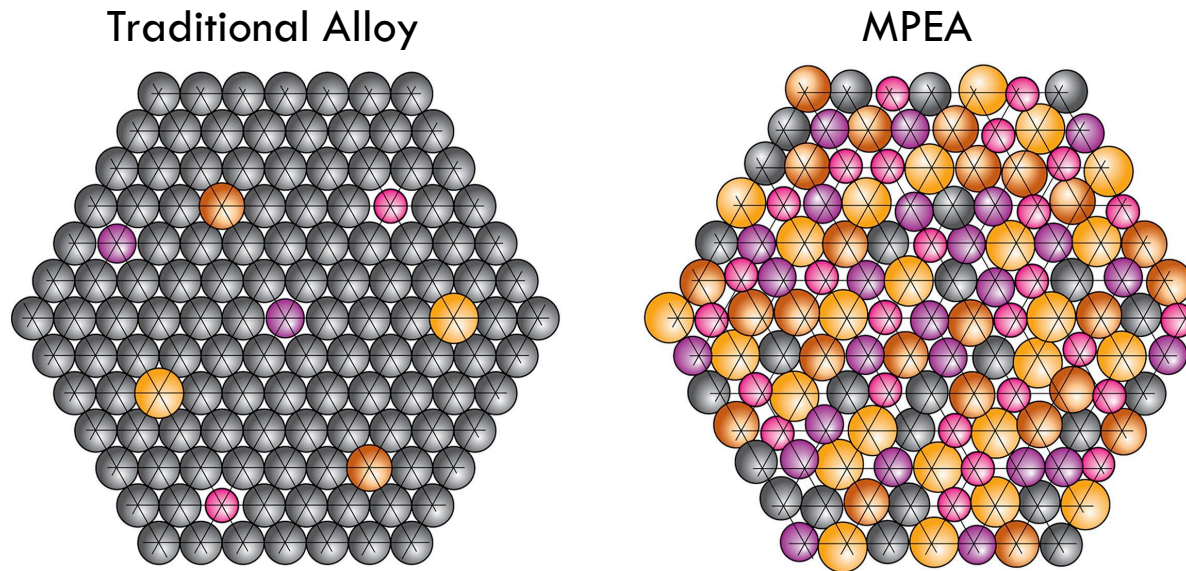
**Part I: Refractory Multi-Principal Element Alloys**

**Part II: Interstitial Elements in Refractory Alloys**

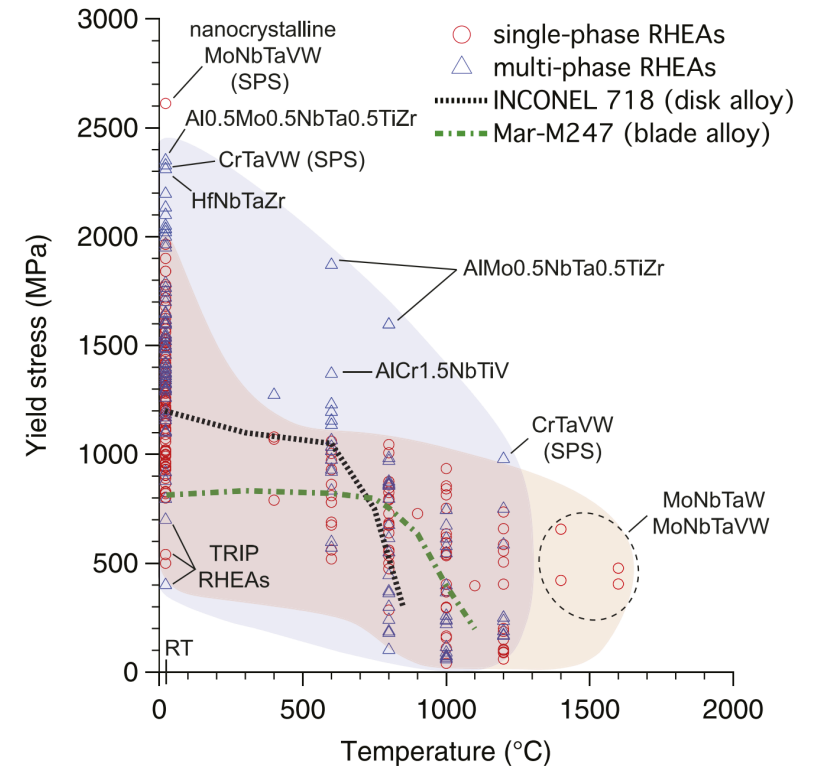
# What are multi-principal element alloys?

22 <b>Ti</b> Titanium 47.867	23 <b>V</b> Vanadium 50.942	24 <b>Cr</b> Chromium 51.996
40 <b>Zr</b> Zirconium 91.224	41 <b>Nb</b> Niobium 92.906	42 <b>Mo</b> Molybdenum 95.95
72 <b>Hf</b> Hafnium 178.49	73 <b>Ta</b> Tantalum 180.948	74 <b>W</b> Tungsten 183.84

- Composed of several element types with no dominant species
- Combination of high strength and toughness
- Huge, unexplored composition space



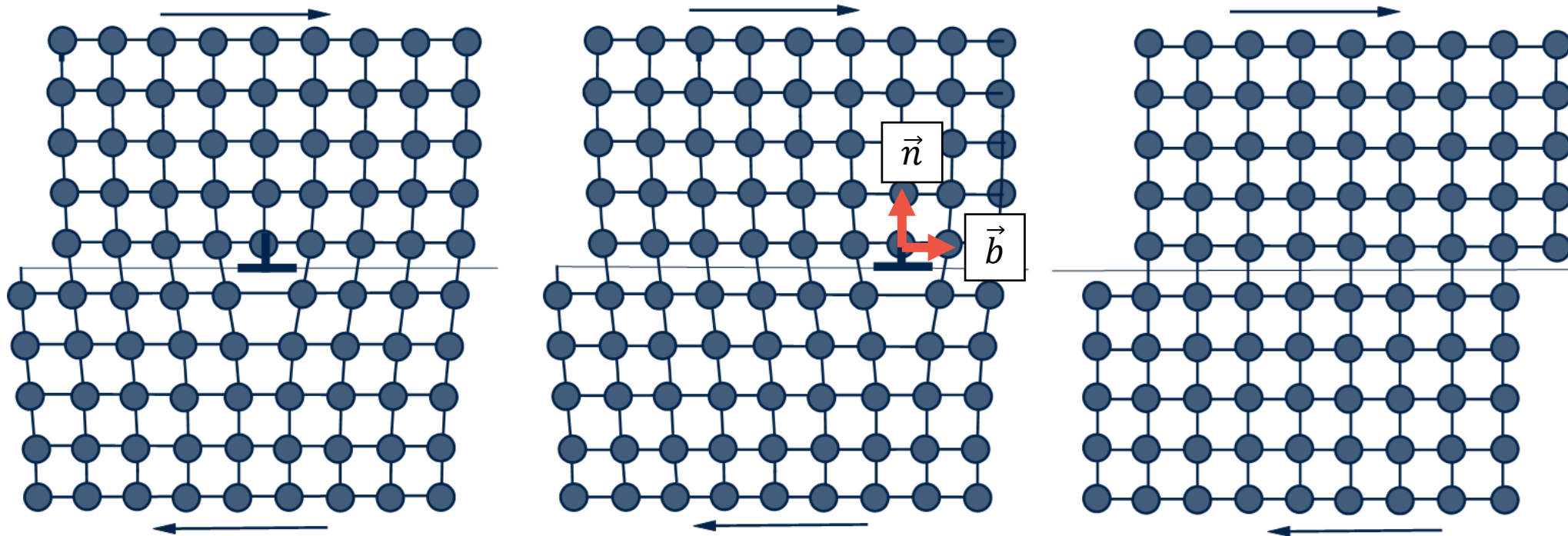
Miracle et al. *Acta Mater*, 122:448-511, 2017.



Senkov, O. N. et al. (2018). *J. Mater. Res.*, 33(19), 3092-3128.

# Dislocations control plastic deformation

- Dislocations are defined by their Burgers vector, line direction, and slip plane



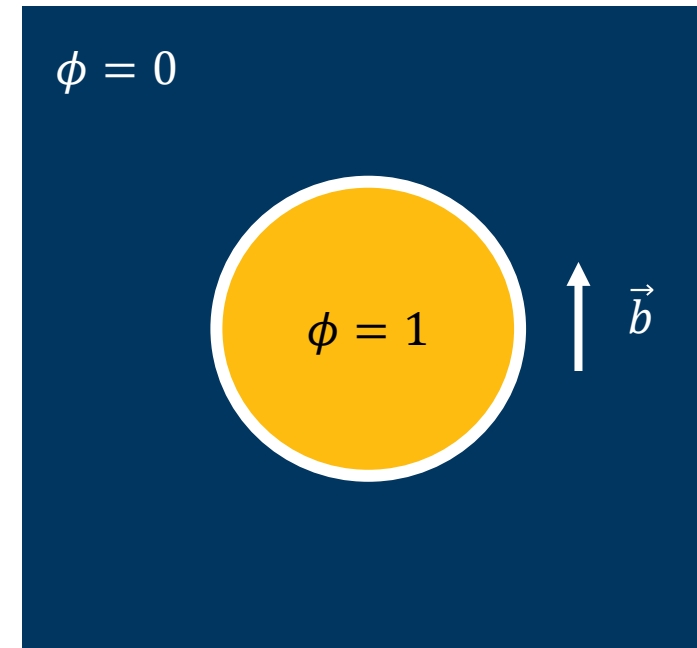
Cai, W., & Nix, W. D. (2016). *Imperfections in Crystalline Solids*.

Screw dislocation:  $\vec{b}$  parallel to line direction

Edge dislocation:  $\vec{b}$  orthogonal to line direction

# Phase-field dislocation dynamics

- Mesoscale, energy-based dislocation model
- Computationally efficient, can run large numbers of simulations
- Uses scalar order parameters ( $\phi$ ) to track dislocation structure
  - $\phi = 0$ : Unslipped
  - $\phi = 1$ : Slipped
  - $0 < \phi < 1$ : Dislocation



$$E = E_{elas} + E_{ext} + E_{lattice}$$

Elastic interaction energy

Externally applied energy

Energy to break bonds  
(material specific)

$$E_{elas}(\phi) = \frac{1}{2} [\epsilon - \epsilon^p(\phi)] \cdot C [\epsilon - \epsilon^p(\phi)]$$

$$E_{ext}(\phi) = \sigma^{app} \cdot \epsilon^p(\phi)$$

$$E_{lattice}(\phi) = \frac{E_{USFE}}{d_{slip}} \sin^2 \pi \phi$$

$$\epsilon^p(\phi) = \frac{b\phi}{2d} (s \otimes n + n \otimes s)$$

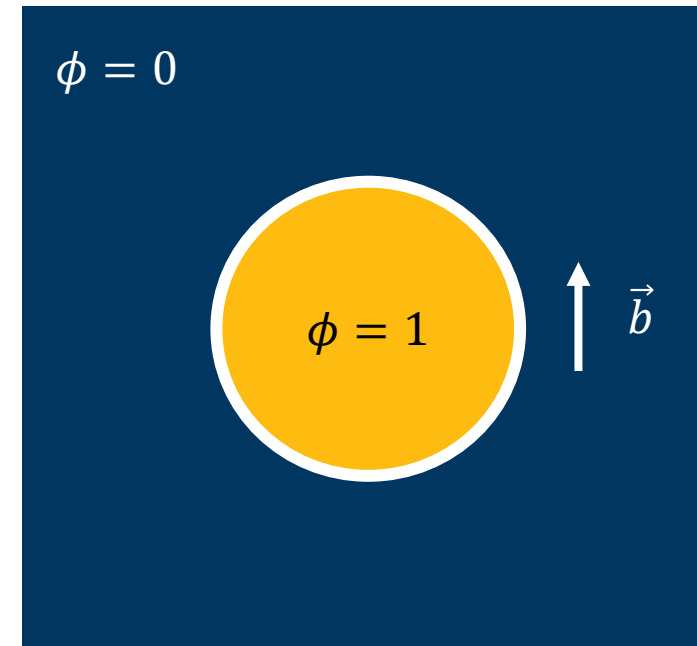
# Phase-field dislocation dynamics

- Mesoscale, energy-based dislocation model
- Computationally efficient, can run large numbers of simulations
- Uses scalar order parameters ( $\phi$ ) to track dislocation structure
  - $\phi = 0$ : Unslipped
  - $\phi = 1$ : Slipped
  - $0 < \phi < 1$ : Dislocation

$$E = E_{elas} + E_{ext} + E_{lattice}$$

Total energy minimized with Ginzburg-Landau Equation

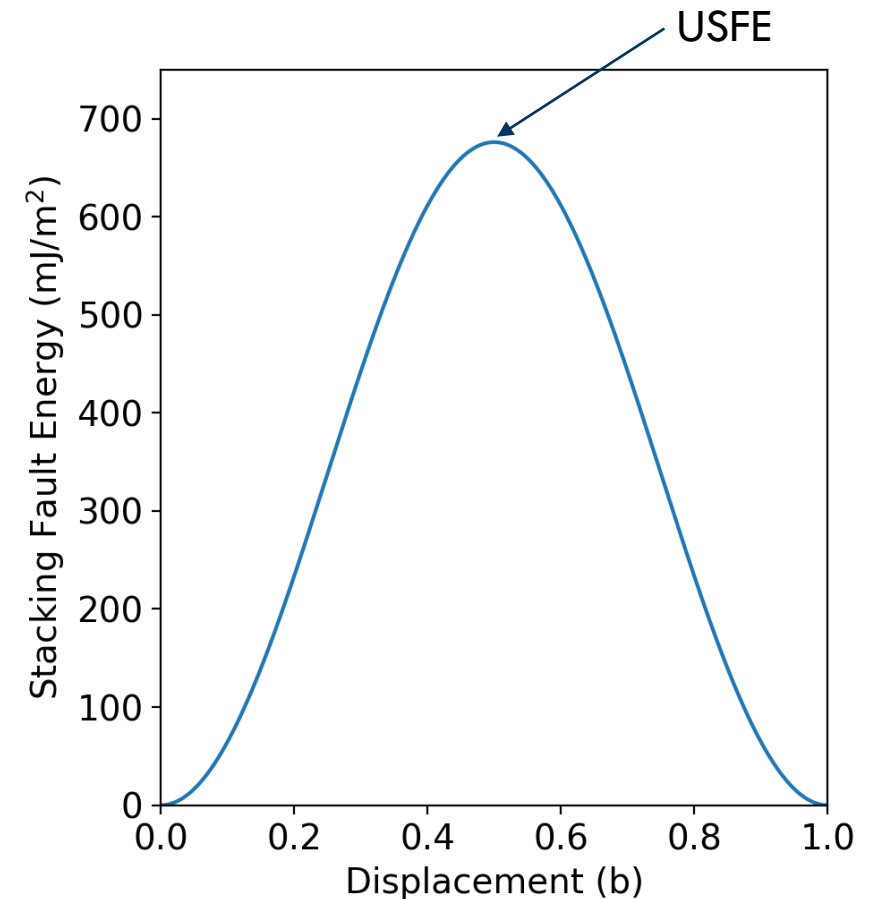
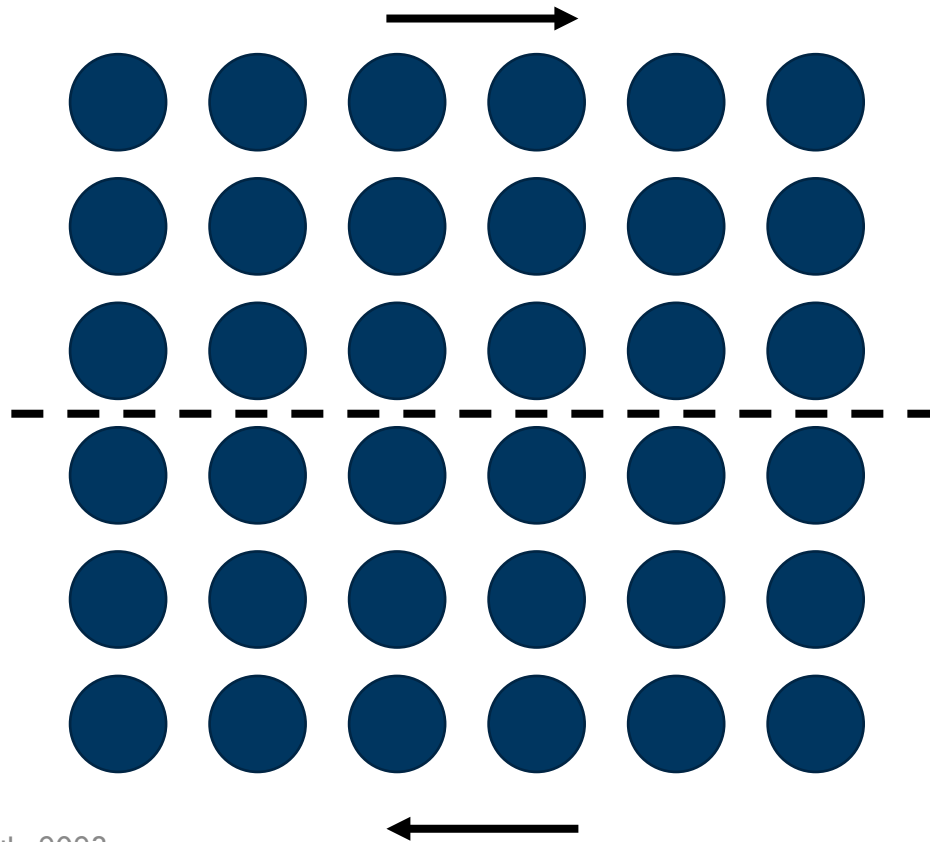
$$\boxed{\frac{d\phi}{dt} = -m_{disl} \frac{\partial E}{\partial \phi}}$$





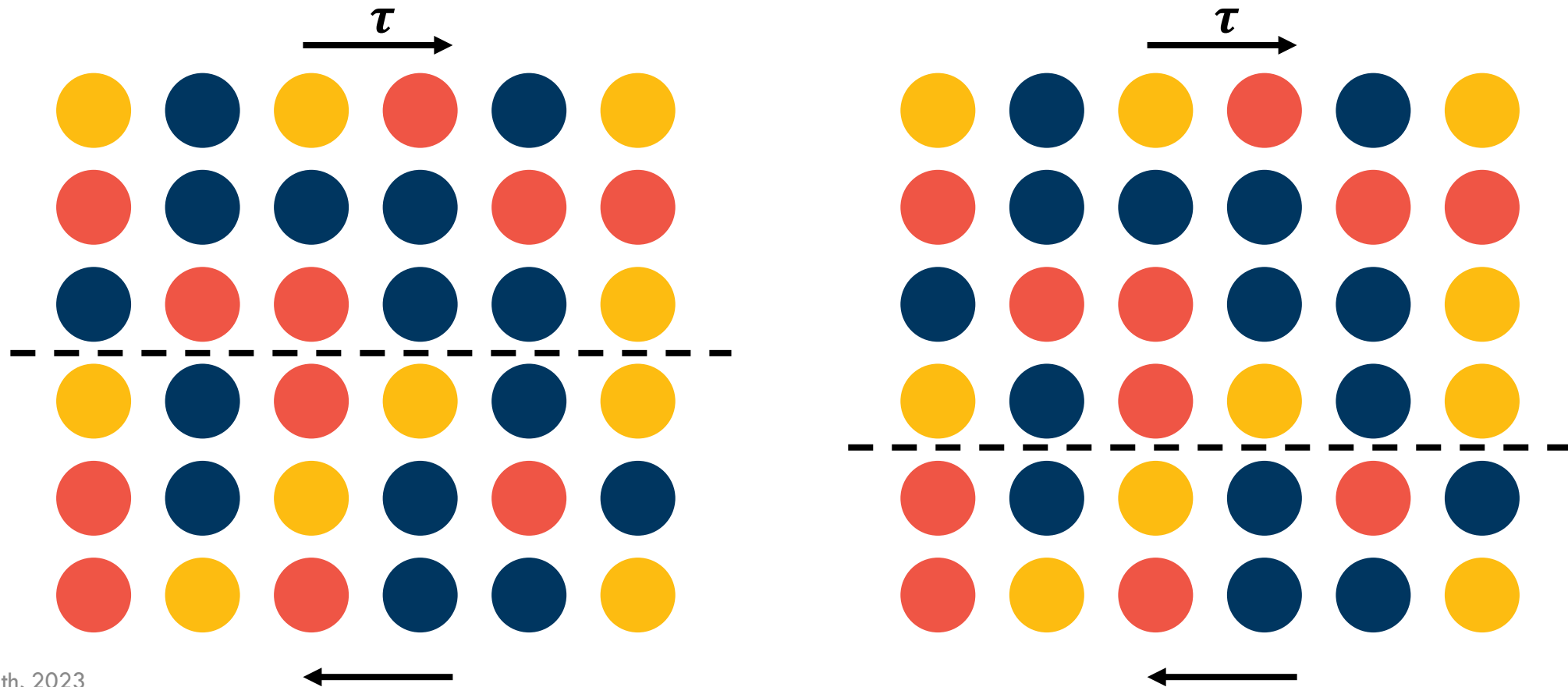
# Unstable stacking fault energy (USFE)

- USFE measures energy required to break bonds across the slip plane
- Used to parameterize lattice energy in PFDD



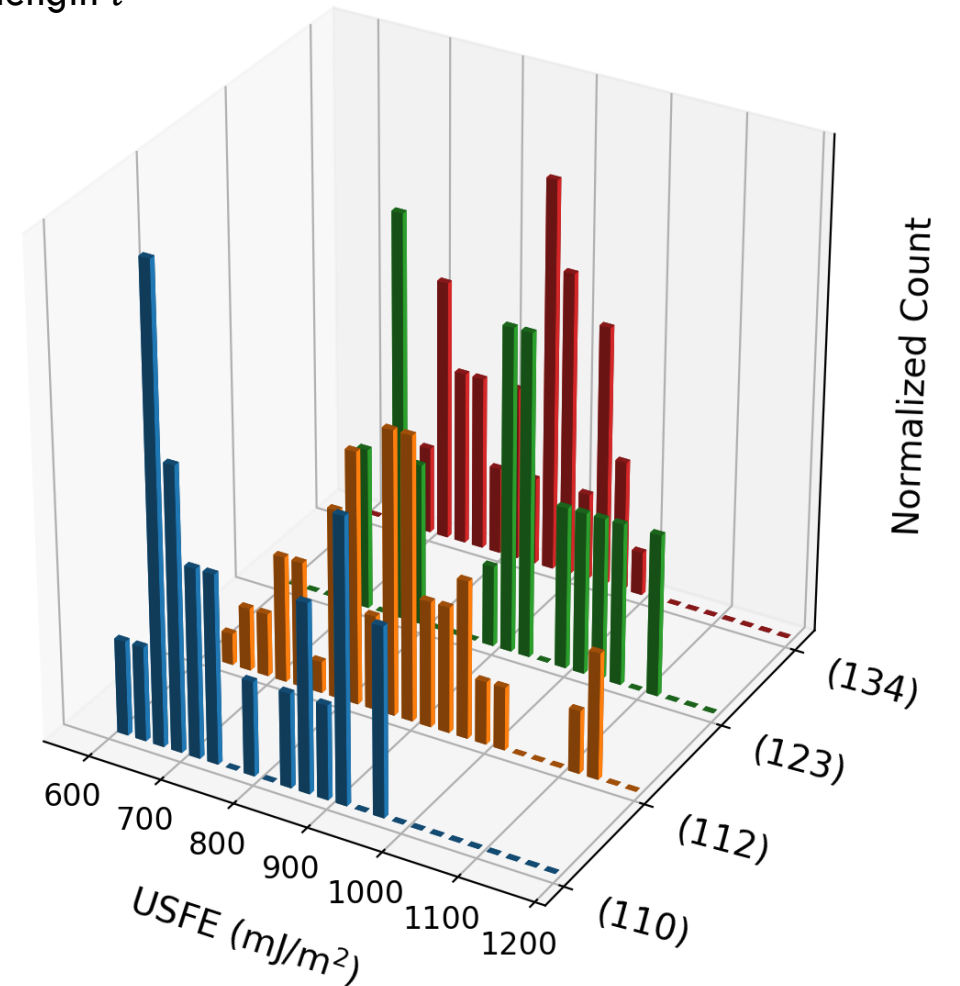
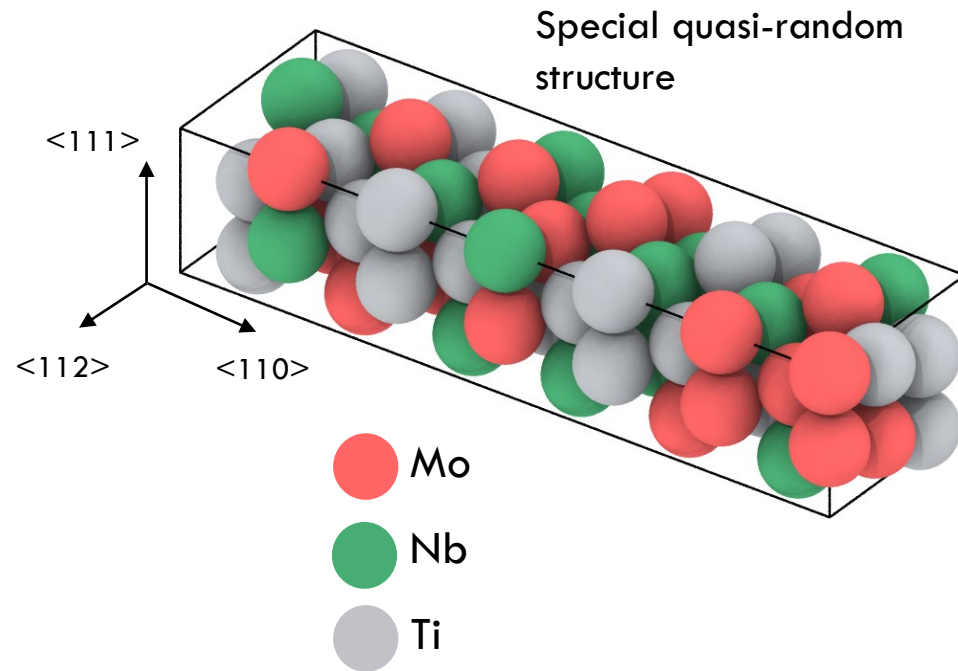
# Unstable stacking fault energy in an MPEA

- MPEAs have a disordered lattice
- Local USFE will vary depending on composition and local atomic configurations

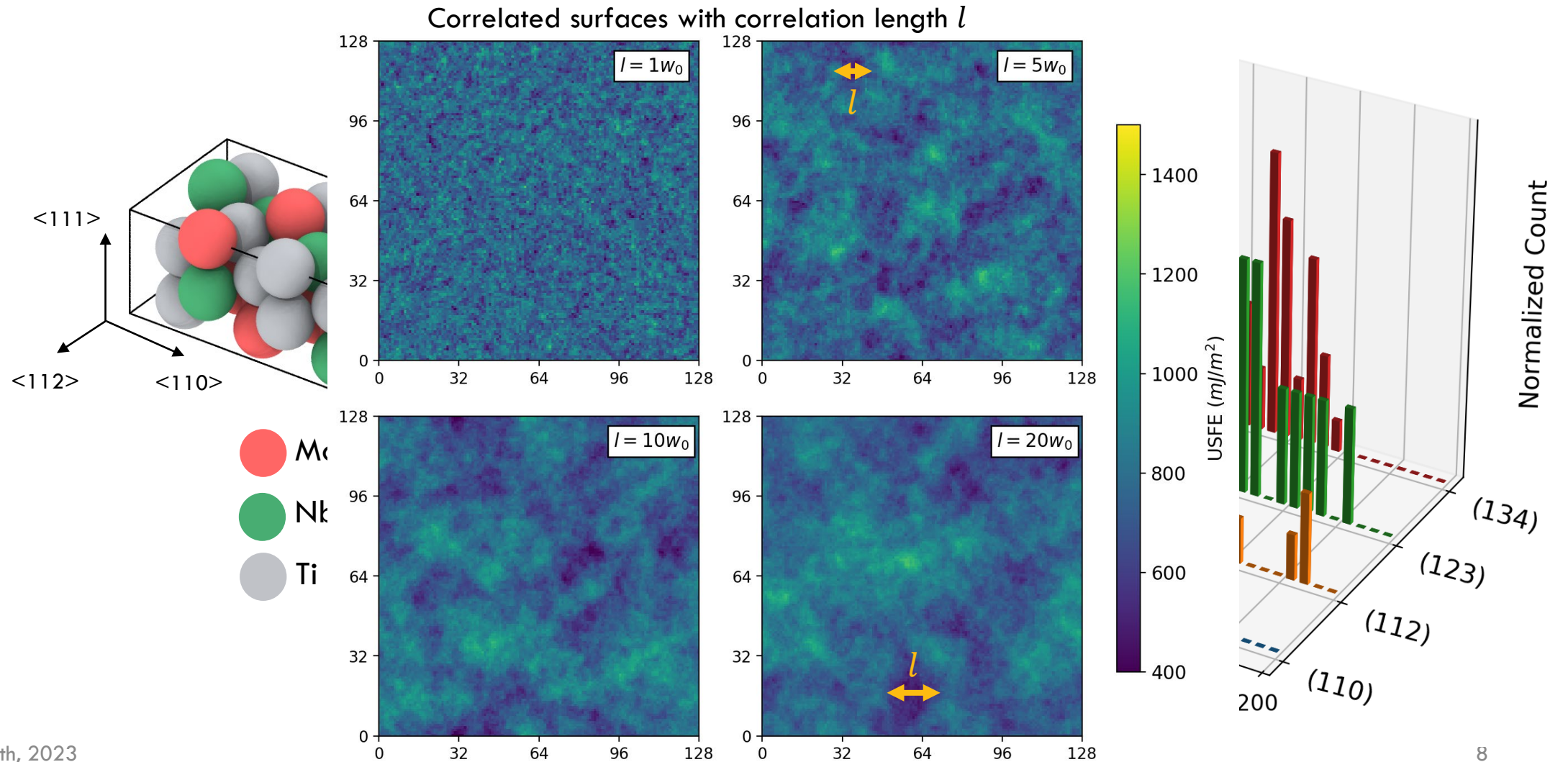


# Unstable stacking fault energy – MoNbTi

Correlated surfaces with correlation length  $l$

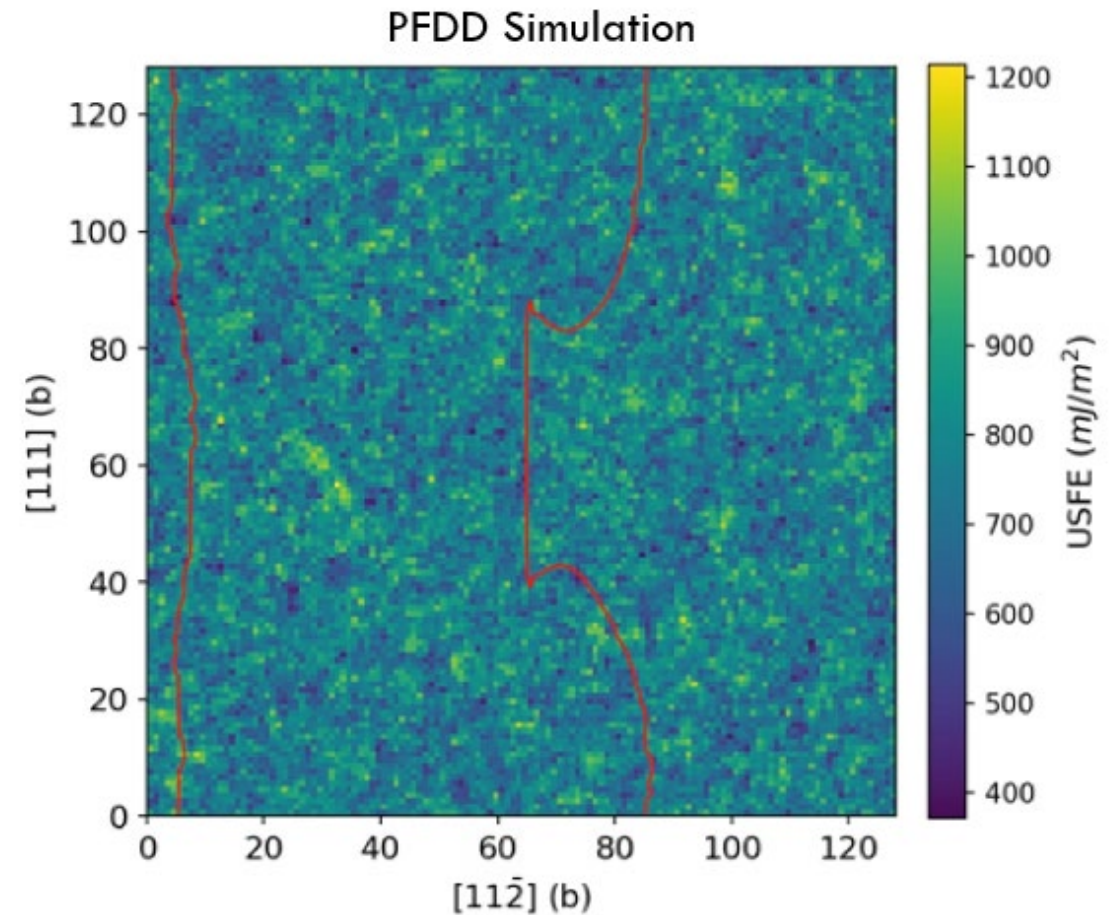
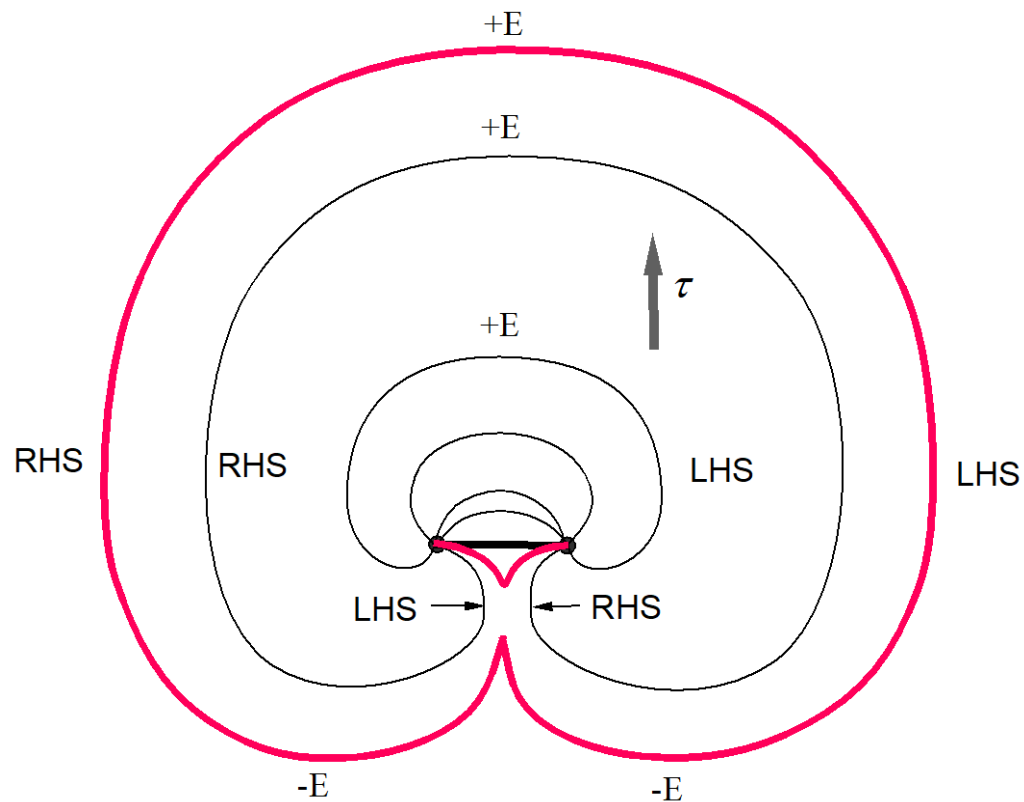


# Unstable stacking fault energy – MoNbTi



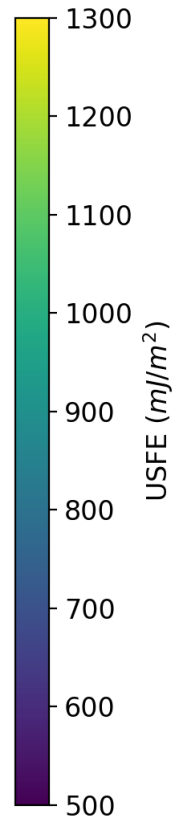
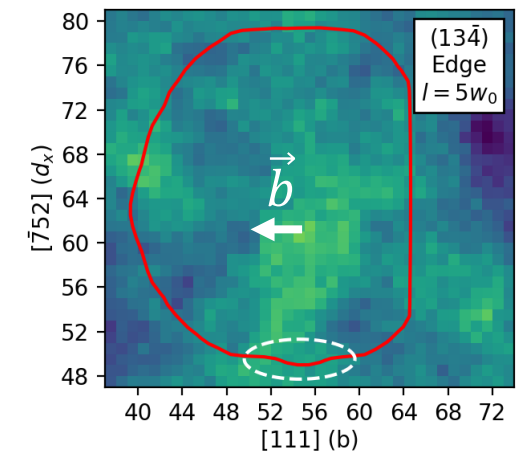
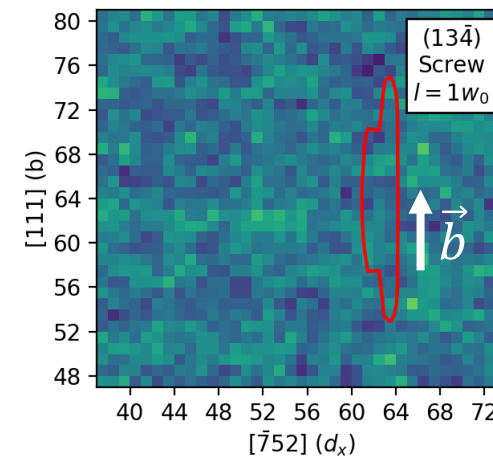
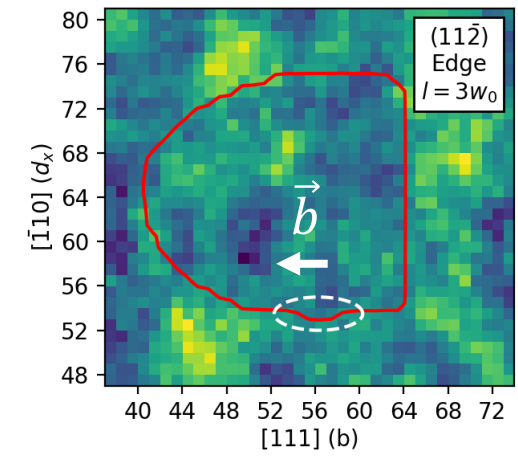
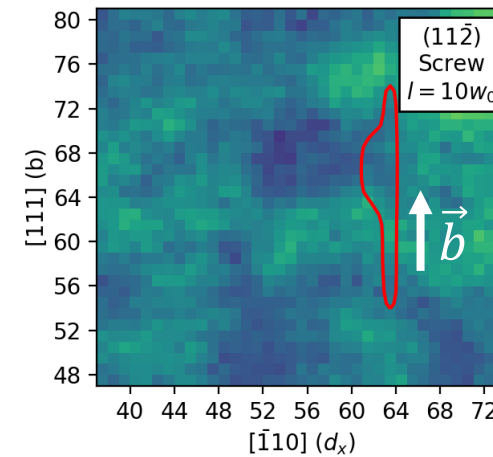
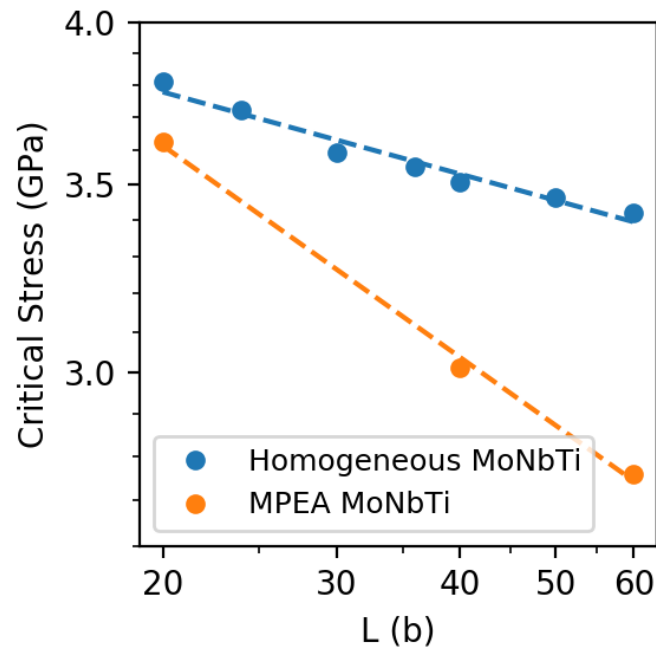
# Simulating dislocation multiplication

Frank-Read sources are common mechanism for dislocation generation



# Frank-Read source activation mechanism

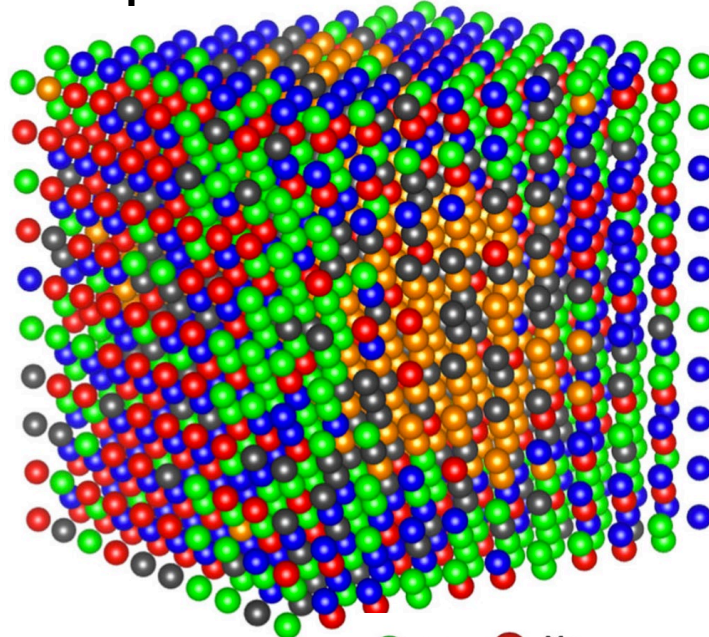
- Both screw and edge sources are controlled by kink-pair nucleation into low USFE regions
- Change in mechanism causes more severe scaling with Frank-Read source length



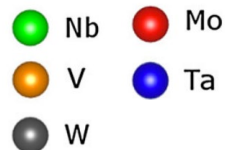
# The role of short-range order in MPEAs

MPEA lattices are disordered in the long-range, but there is thermodynamically driven local order

MoNbTaVW Equilibrium Structure at 400K



Fernández-Caballero  
et al. *J Phase Equilib Diff*,  
38:391-403, 2017.



## TaNbTi

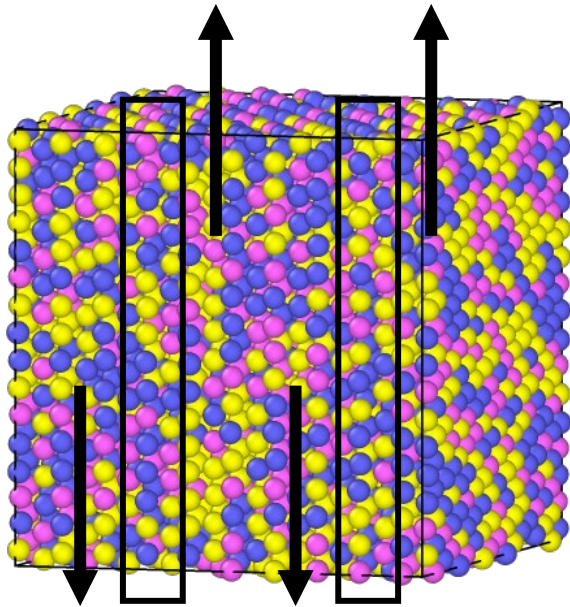
- Less SRO

## MoNbTi

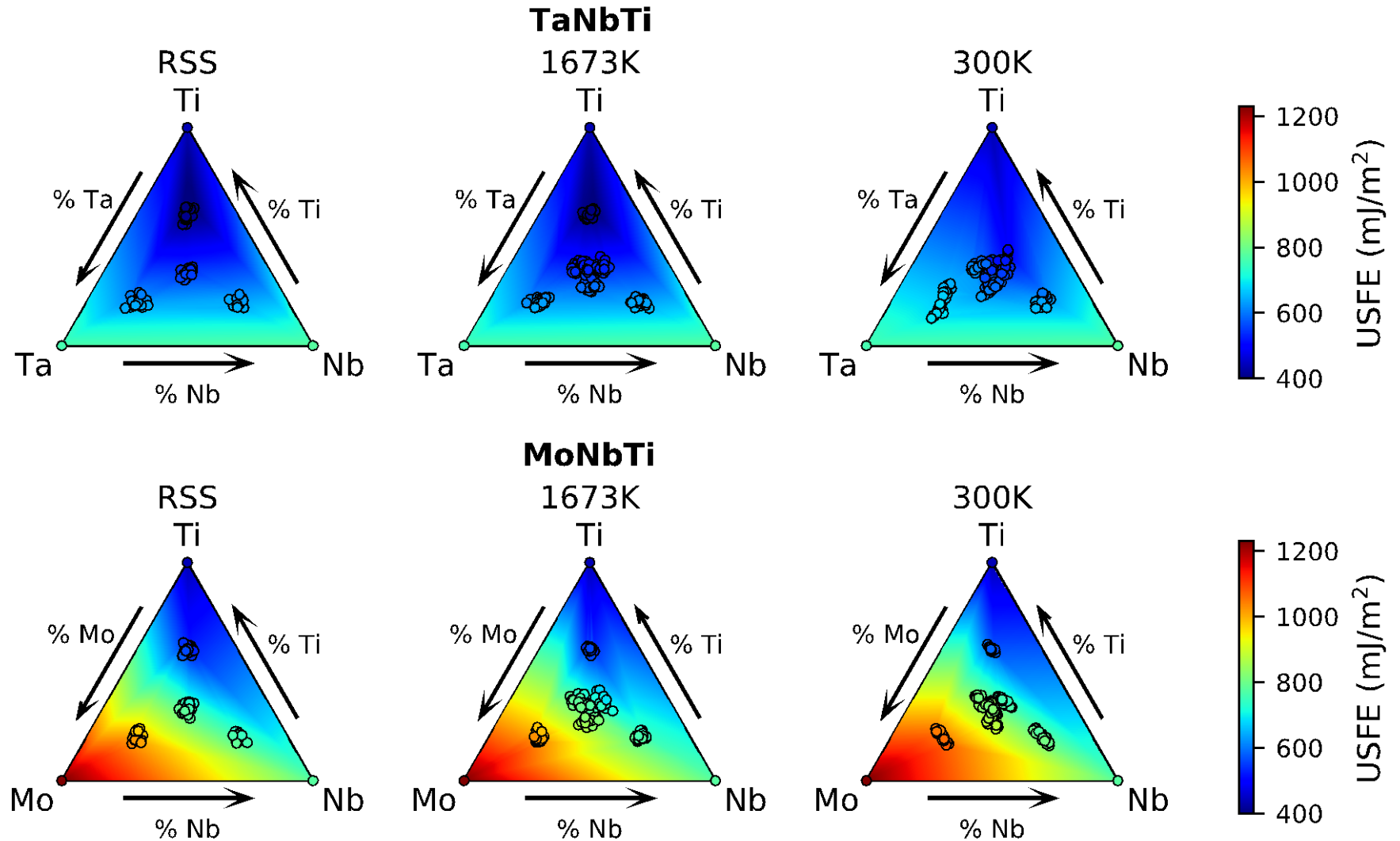
- More SRO

22 <b>Ti</b> Titanium 47.867	23 <b>V</b> Vanadium 50.942	24 <b>Cr</b> Chromium 51.996
40 <b>Zr</b> Zirconium 91.224	41 <b>Nb</b> Niobium 92.906	42 <b>Mo</b> Molybdenum 95.95
72 <b>Hf</b> Hafnium 178.49	73 <b>Ta</b> Tantalum 180.948	74 <b>W</b> Tungsten 183.84

# Composition-dependent USFE

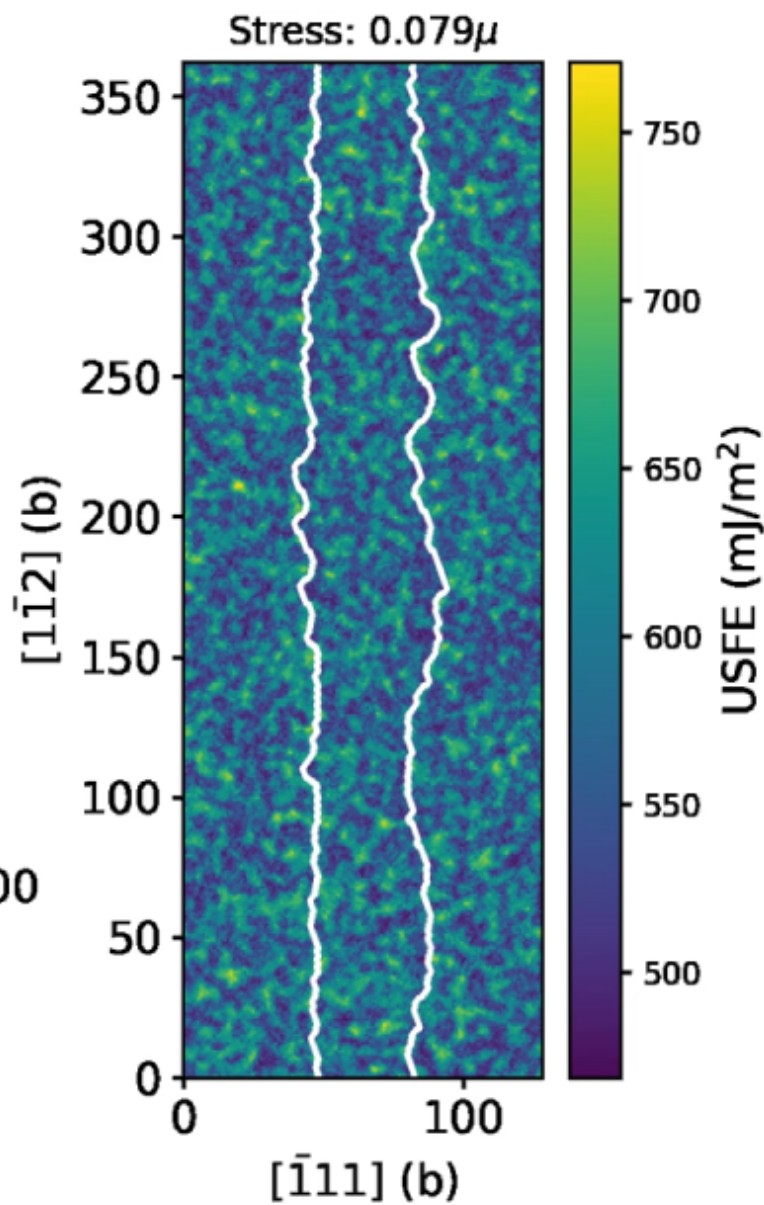
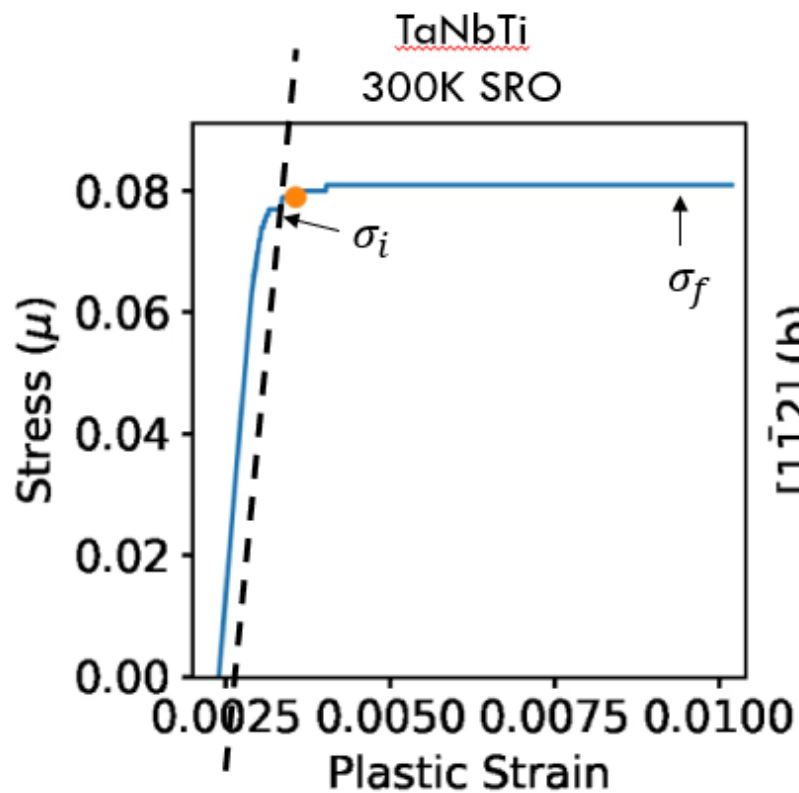


USFE calculated with interatomic potential along different (110) planes with varying local compositions

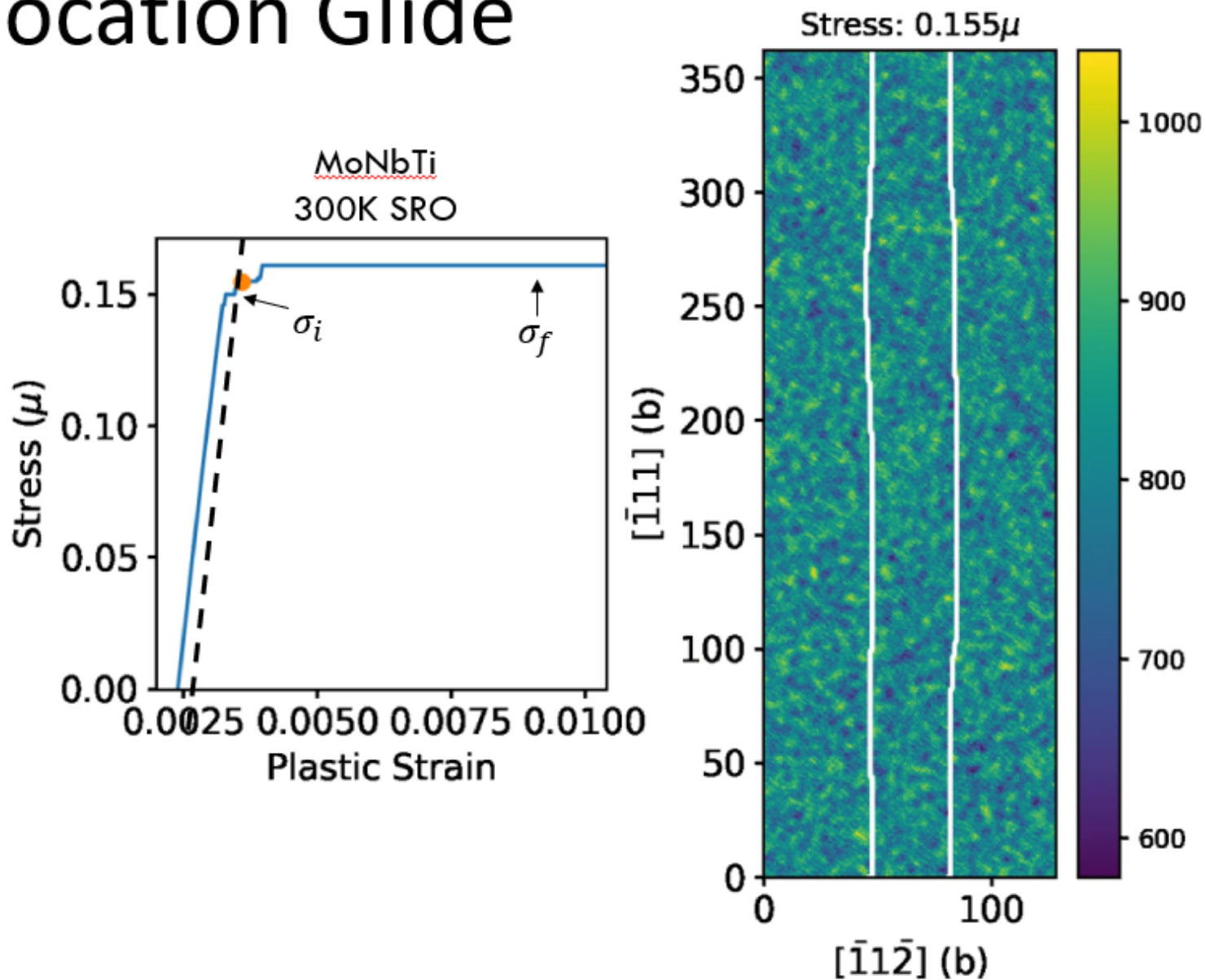




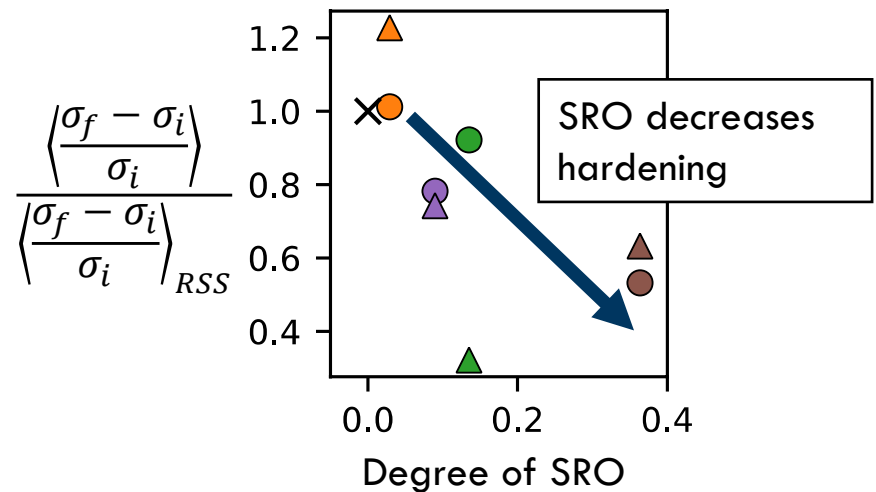
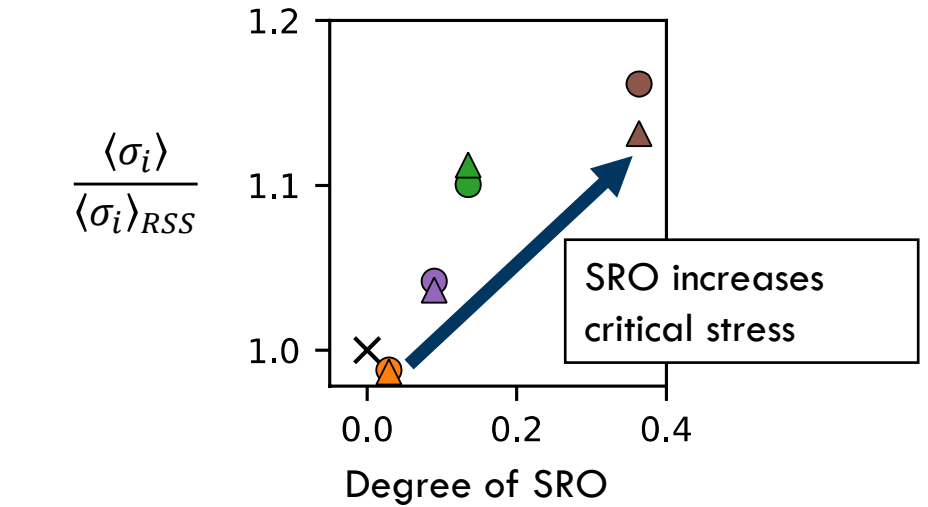
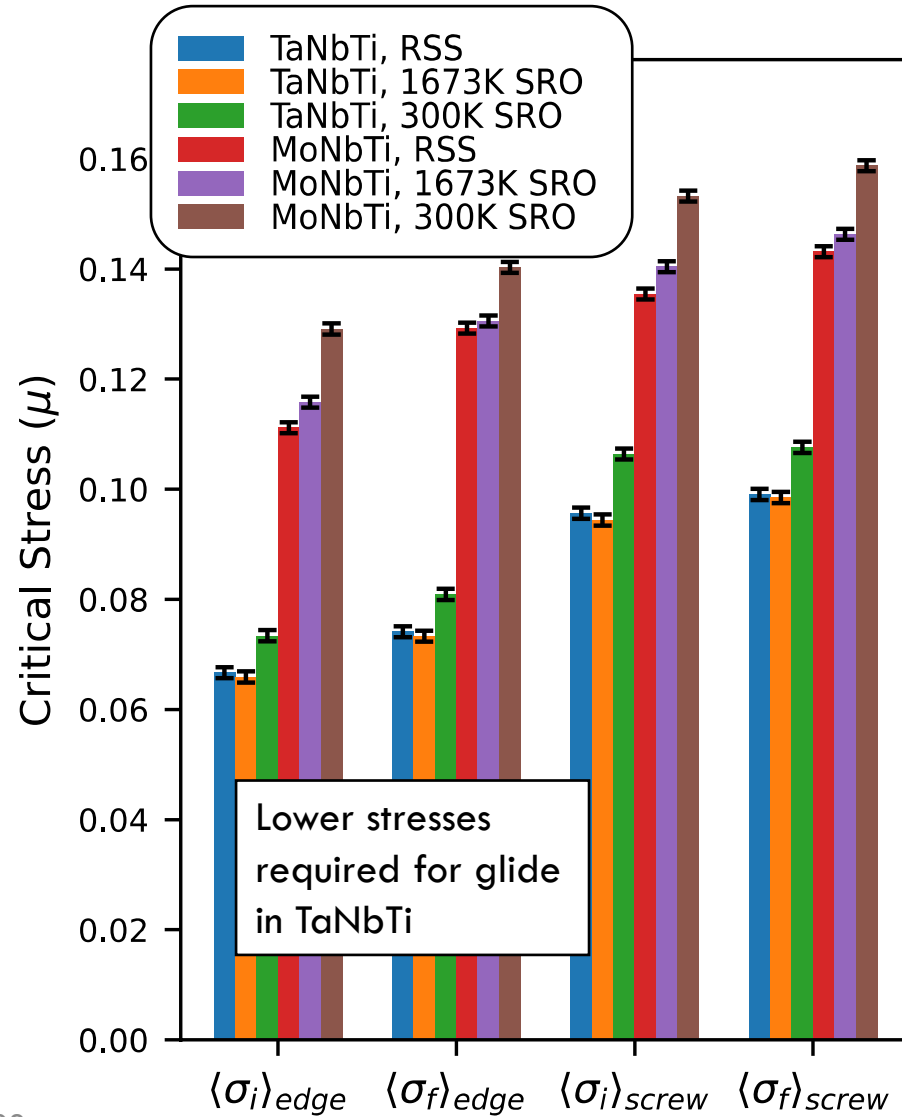
# Edge Dislocation Glide



# Screw Dislocation Glide



# SRO effects on dislocation critical stress



# This talk

**Part I: Refractory Multi-Principal Element Alloys**

**Part II: Interstitial Elements in Refractory Alloys**

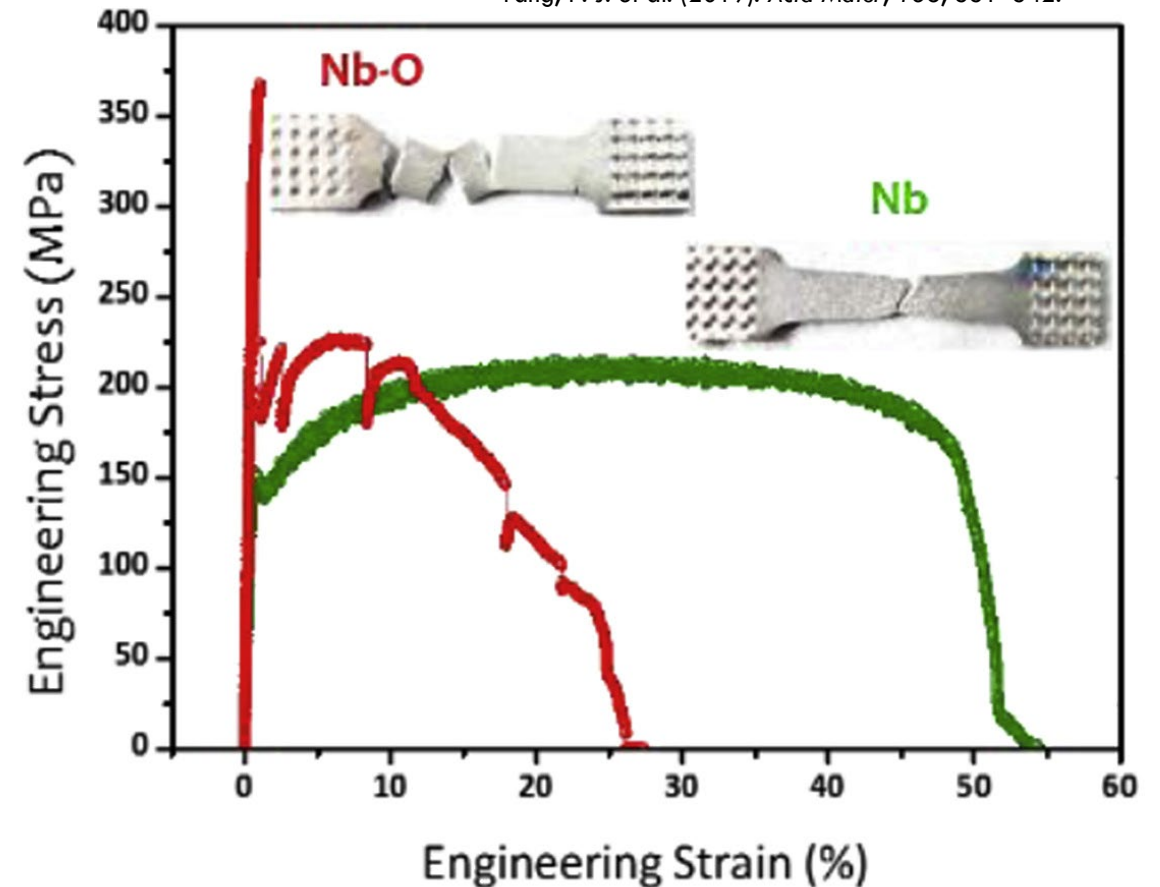
# Problem: Interstitial Embrittlement

- Refractory metals easily absorb interstitial contaminants like O, H, and C from the atmosphere
- Interstitials generally increase yield strength at the expense of ductility

**How do interstitials affect dislocation mechanisms and stresses?**

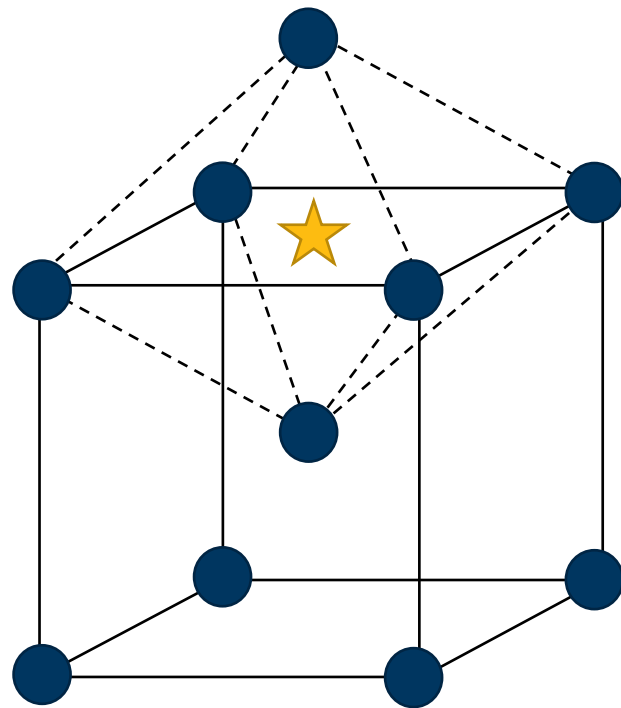
Model systems: Nb-O and W-H

Yang, P. J. et al. (2019). *Acta Mater*, 168, 331–342.

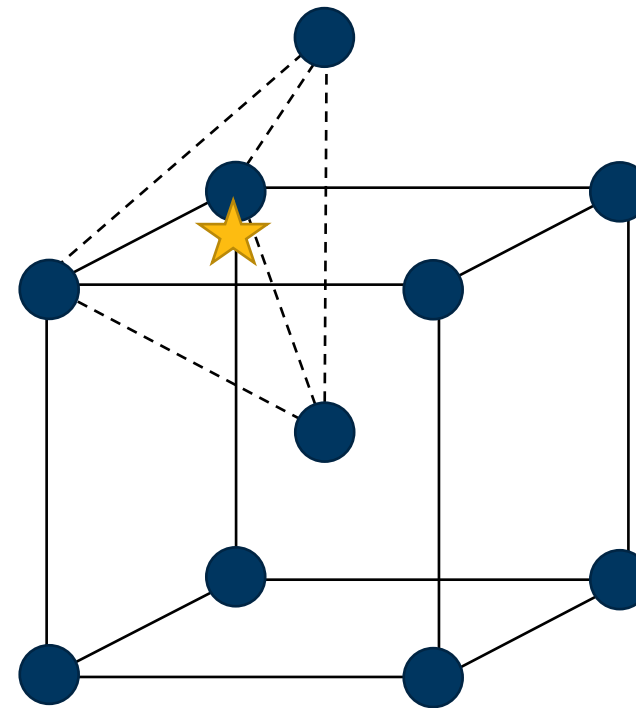


# Interstitials in BCC lattices

- Interstitials create a distortion in the lattice
- Interstitials can interact with dislocations via their stress fields (long-range) or directly at the dislocation core (short-range)



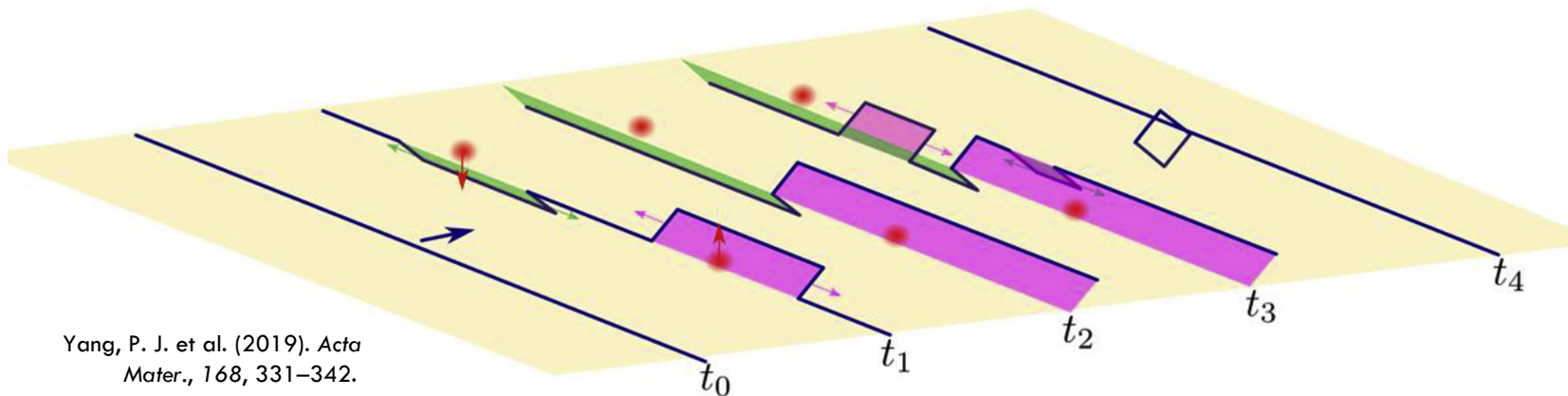
Octahedral site



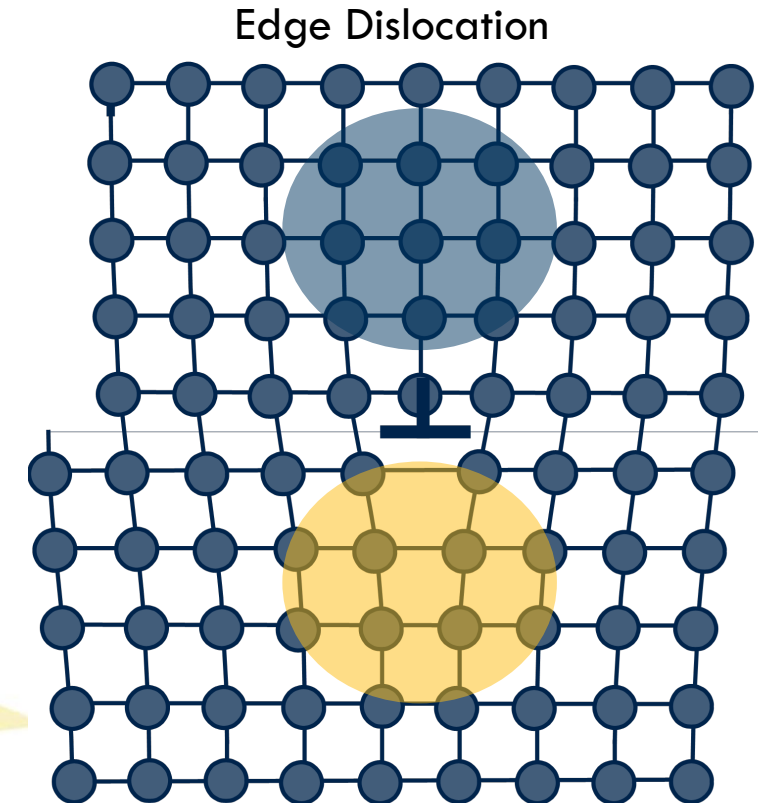
Tetrahedral site

# Long-Range Interactions

- Dislocations have long-range stress fields:  $\sigma \propto \frac{1}{r}$
- Interstitials interact with these stress fields and form atmospheres around dislocation cores
- Interstitials can pin dislocations or cause cross slip and debris formation



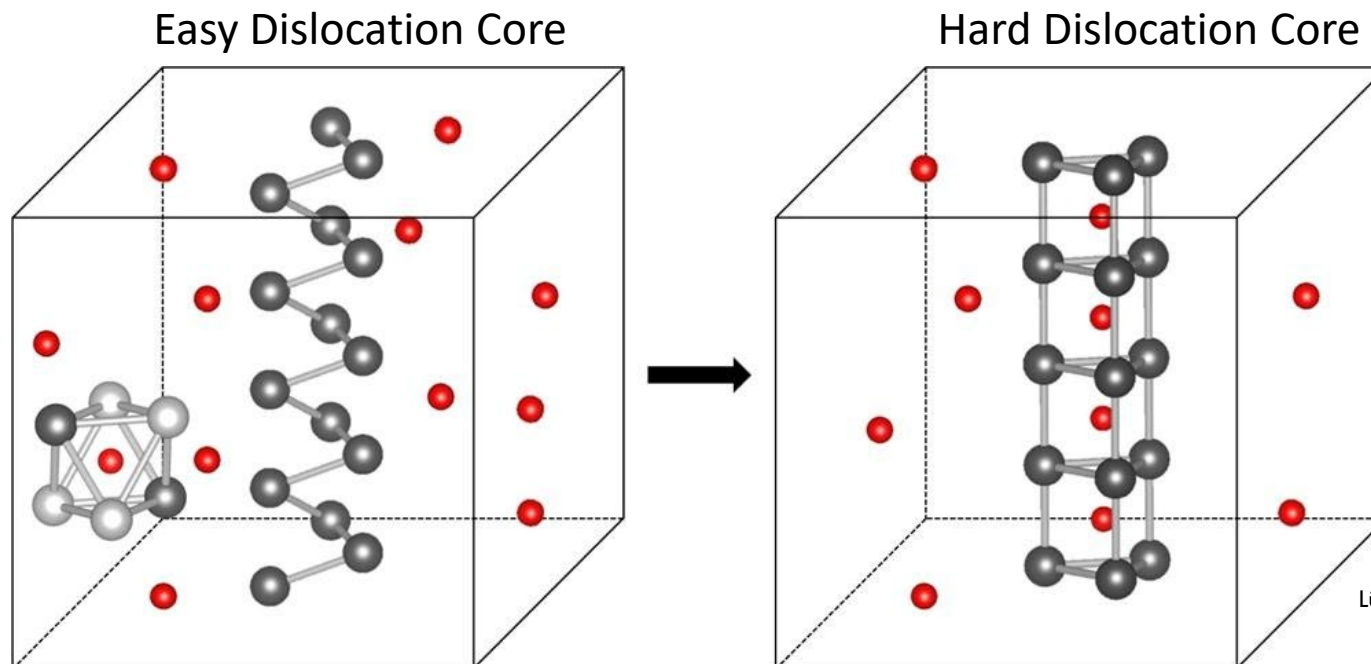
Yang, P. J. et al. (2019). *Acta Mater.*, 168, 331–342.



Cai, W., & Nix, W. D. (2016). *Imperfections in Crystalline Solids*.

# Short-Range Interactions

- Interstitials change the structure and energy of a dislocation core
- Binding energy at dislocation core can pin the dislocation



Lüthi, B. et al. (2018). *Computational Materials Science*, 148, 21–26.



# Interstitials in PFDD

- PFDD tracks dislocation structure through  $\phi$ 
  - $\phi = 0$ : Unslipped
  - $\phi = 1$ : Slipped
  - $0 < \phi < 1$ : Dislocation

$$E = E_{elas} + E_{ext} + E_{lattice}$$

Elastic interaction energy

$$E_{elas}(\phi) = \frac{1}{2} [\epsilon - \epsilon^p(\phi)] \cdot C [\epsilon - \epsilon^p(\phi)]$$

Externally applied energy

$$E_{ext}(\phi) = \sigma^{app} \cdot \epsilon^p(\phi)$$

Energy to break bonds (material specific)

$$E_{lattice}(\phi) = \frac{E_{USFE}}{d_{slip}} \sin^2 \pi \phi$$

# Interstitials in PFDD

- PFDD tracks dislocation structure through  $\phi$ 
  - $\phi = 0$ : Unslipped
  - $\phi = 1$ : Slipped
  - $0 < \phi < 1$ : Dislocation
- Add a new parameter  $c$  to track local interstitial concentration

$$E = E_{elas} + E_{ext} + E_{lattice}$$

Elastic interaction energy

$$E_{elas}(\phi, c) = \frac{1}{2} [\epsilon - \epsilon^p(\phi) - \epsilon^{int}(c)] \cdot C [\epsilon - \epsilon^p(\phi) - \epsilon^{int}(c)]$$

Long-range, elastic interactions

Externally applied energy

$$E_{ext}(\phi) = \sigma^{app} \cdot \epsilon^p(\phi)$$

Energy to break bonds  
(material specific)

$$E_{lattice}(\phi, c) = \frac{E_{USFE}(c)}{d_{slip}} \sin^2 \pi \phi$$

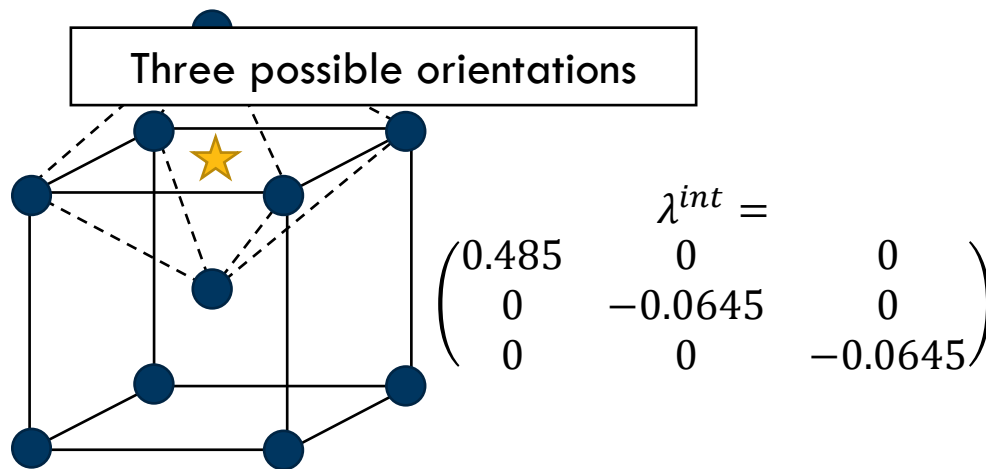
Short-range, core interactions

# Long-range interactions in PFDD

$$E_{elas}(\phi, c) = \frac{1}{2} [\epsilon - \epsilon^p(\phi) - \epsilon^{int}(c)] \cdot C [\epsilon - \epsilon^p(\phi) - \epsilon^{int}(c)]$$

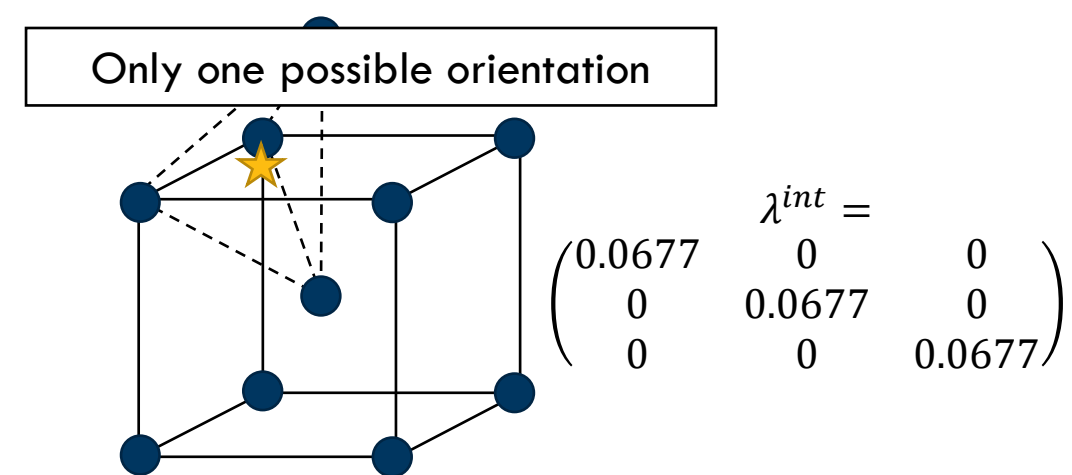
- Interstitial strain given by  $\epsilon^{int}(c) = \lambda^{int} c$ 
  - $\lambda^{int}$  determined from experiments or atomistic calculations

**Nb-O**



O occupies octahedral sites

**W-H**



H occupies tetrahedral sites

# Short-range interactions in PFDD

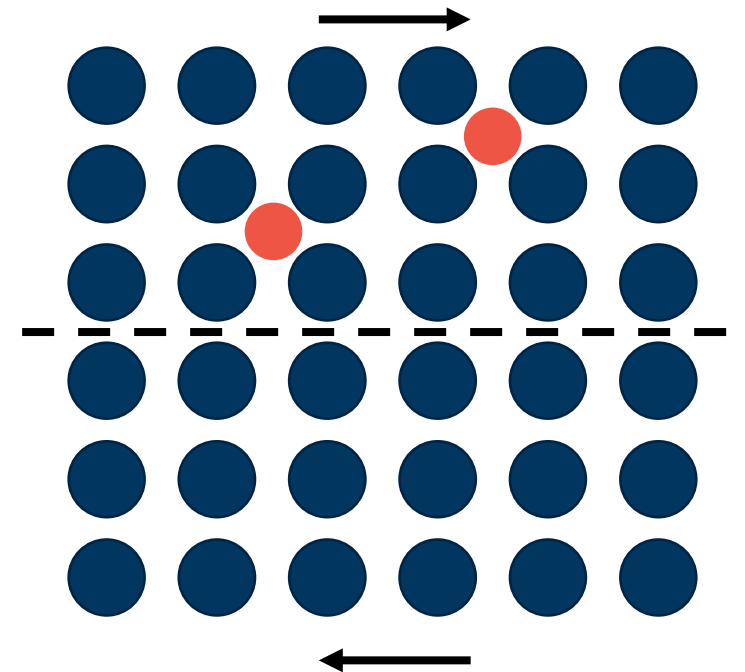
$$E_{lattice}(\phi, c) = \frac{E_{USFE}(c)}{d_{slip}} \sin^2 \pi \phi$$

- Need to calculate USFE for different interstitial concentrations
- Idea: calculate interaction energy of different interstitial sites
  - $E_{int-SF}$ : change in stacking fault energy due to interstitial

$$E_{USFE}(c) = E_{USFE}(0) + \sum_A \frac{c^i E_{int-SF}^i}{A}$$

Pure metal USFE

Adjustment due to interstitials



# Evolution of concentration in PFDD

Dislocation slip is **non-conserved**:

$$\frac{d\phi}{dt} = -m_{disl} \frac{\partial E}{\partial \phi}$$

Interstitial concentration is **conserved**:

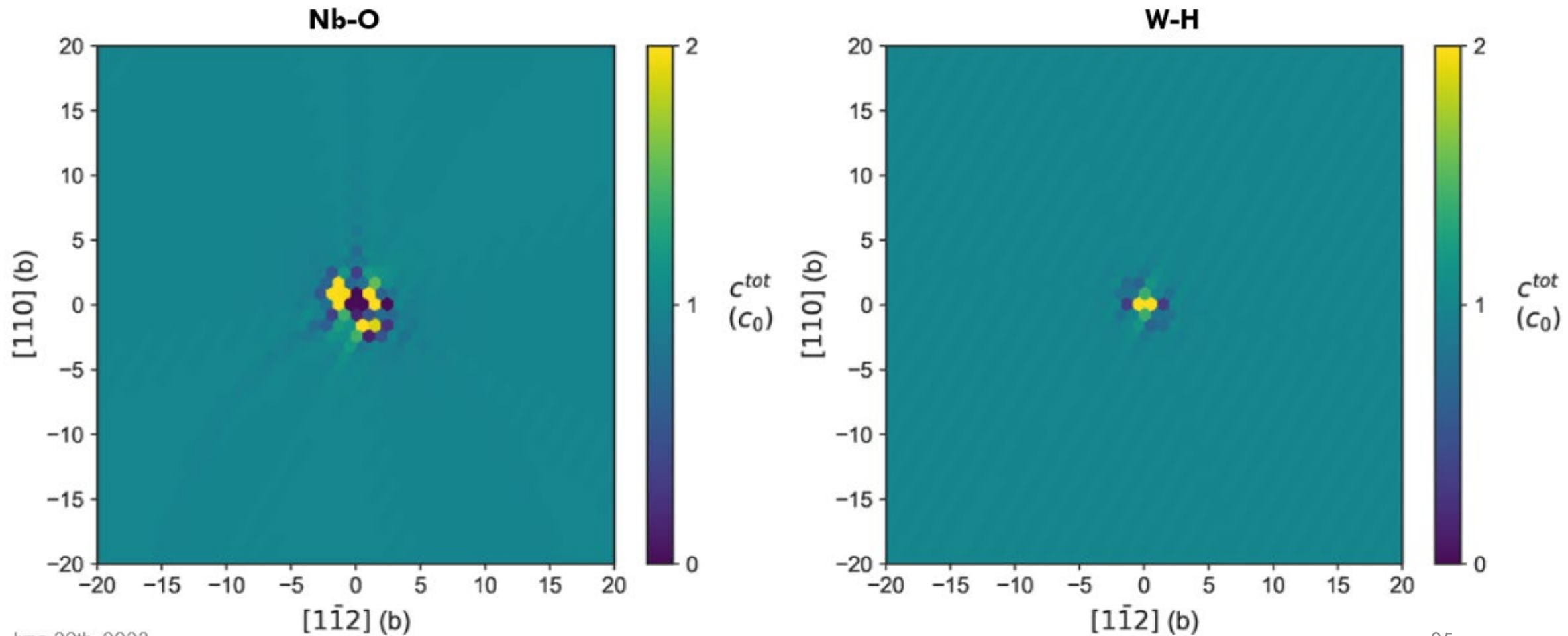
$$\frac{dc}{dt} = \nabla \cdot (m_{int} \nabla \mu)$$

$$\text{Chemical potential: } \mu = \frac{\partial E}{\partial c}$$

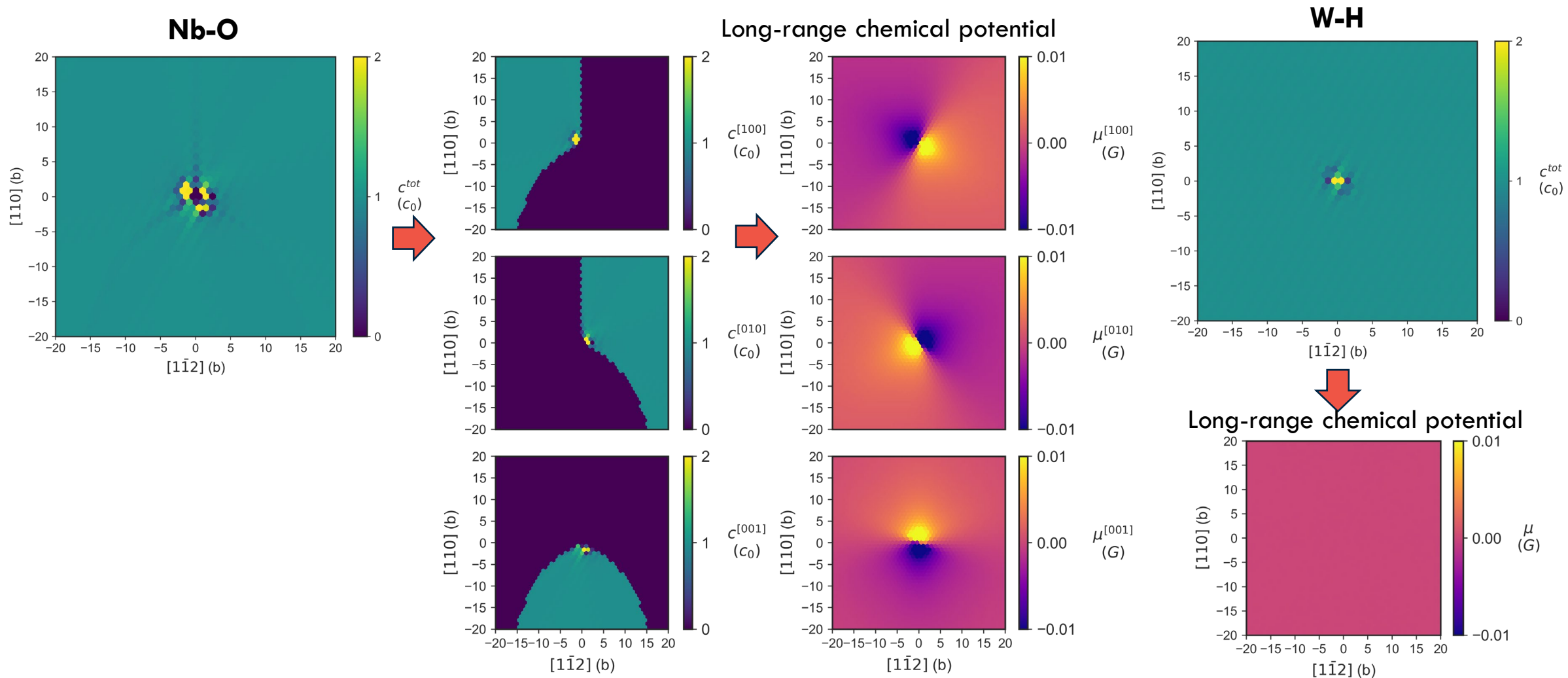
- Interstitials will flow towards lower chemical potential regions
- When there are multiple site types/orientations available, interstitials adopt the lowest energy configuration

# Screw dislocation interstitial atmospheres

Initially homogeneous concentration  $c_0 = 0.01$

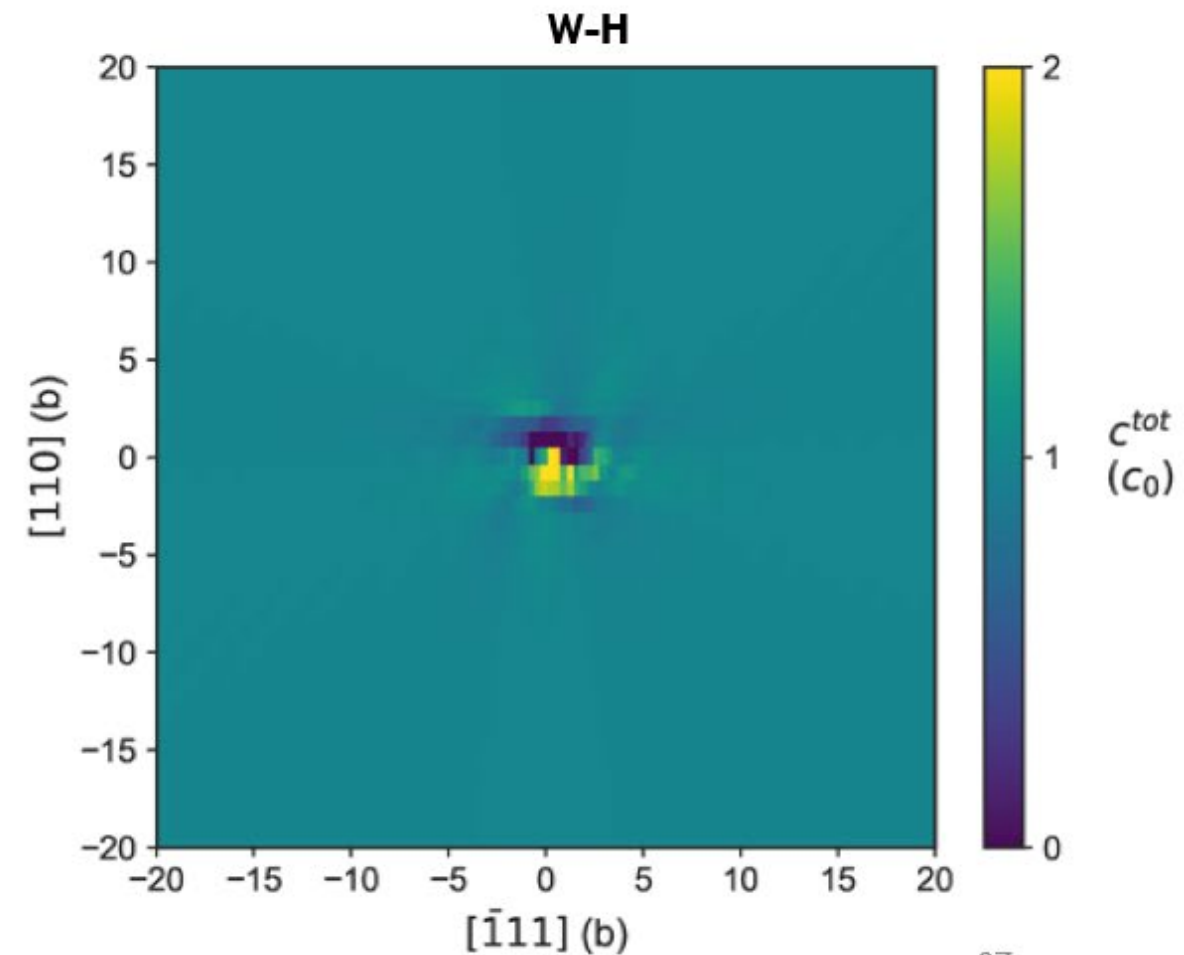
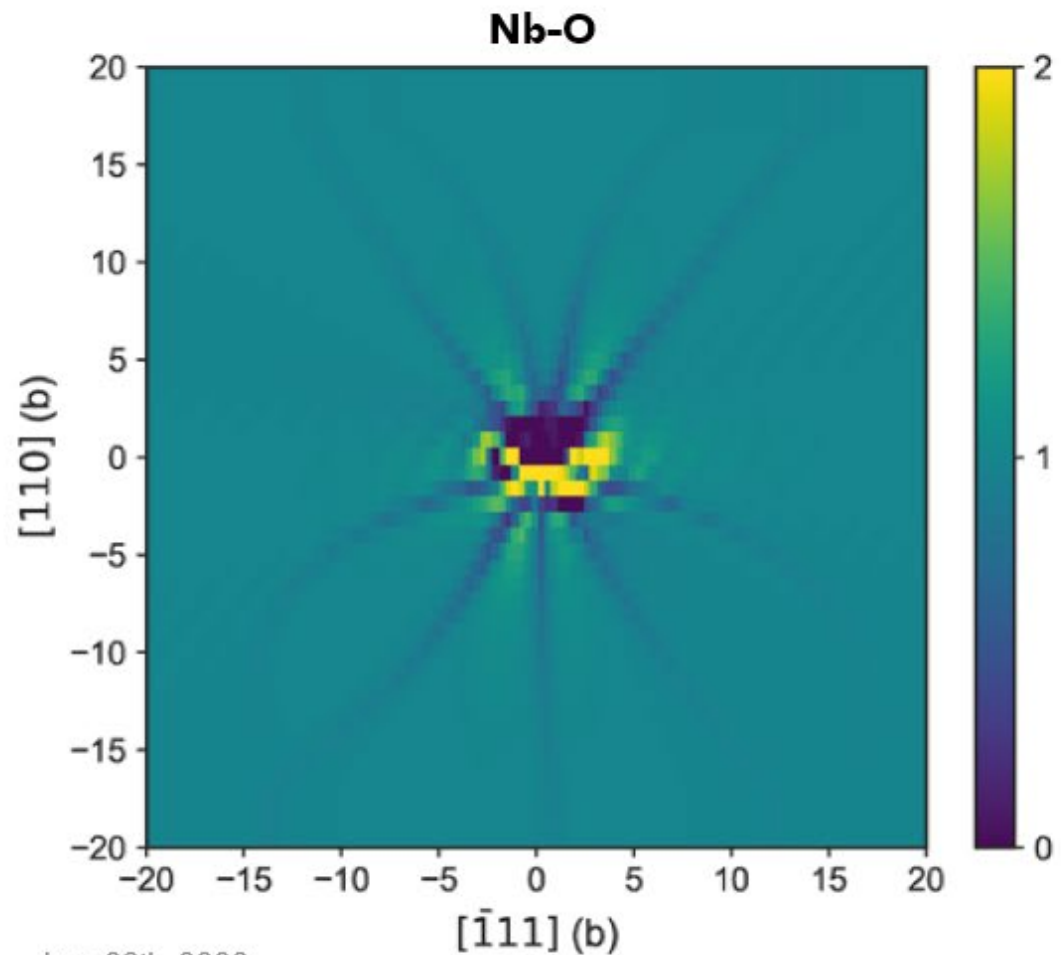


# Screw dislocation interstitial atmospheres



# Edge dislocation interstitial atmospheres

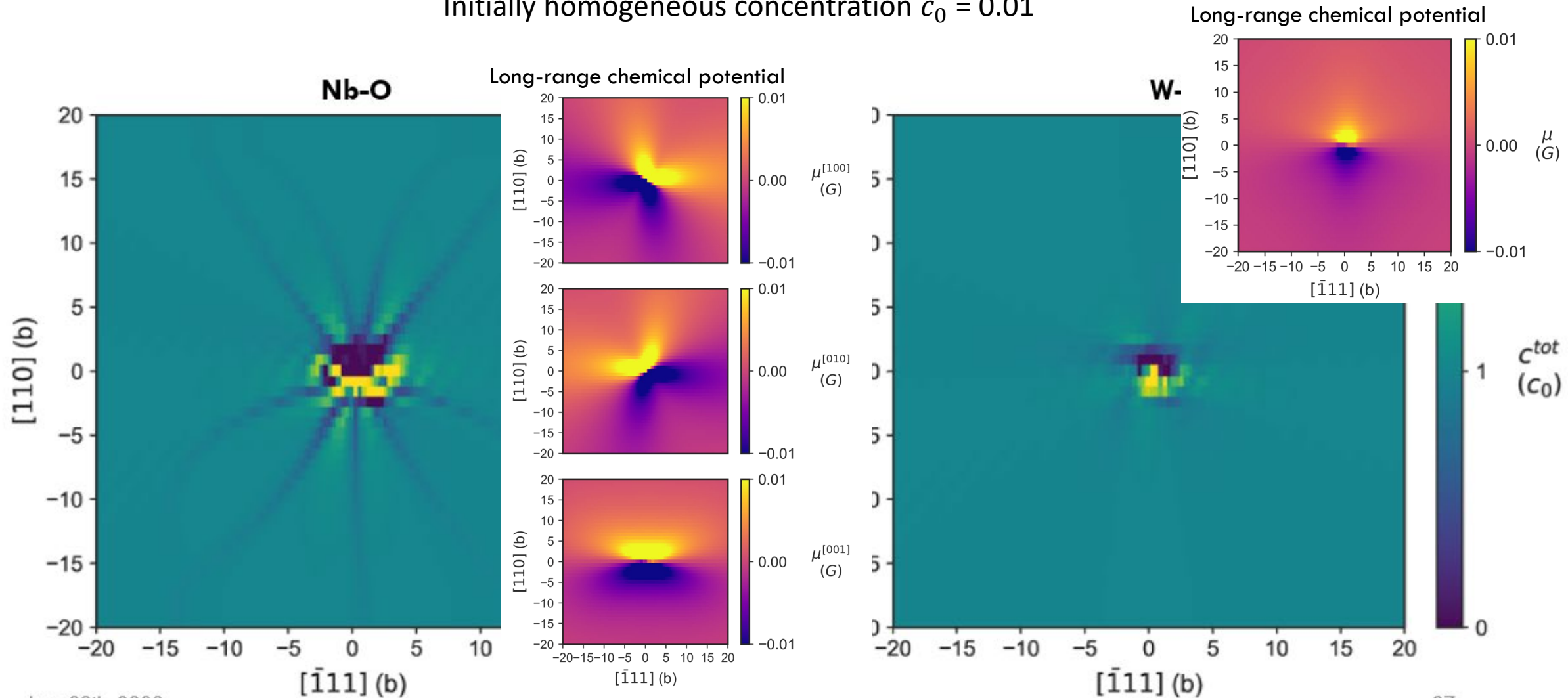
Initially homogeneous concentration  $c_0 = 0.01$





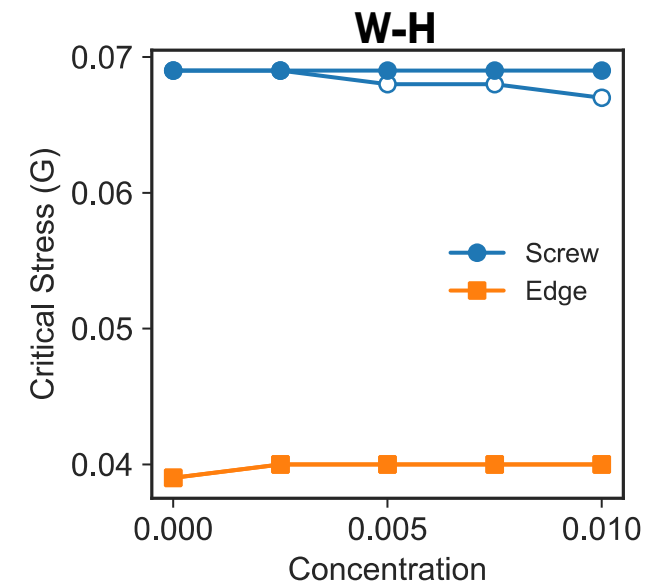
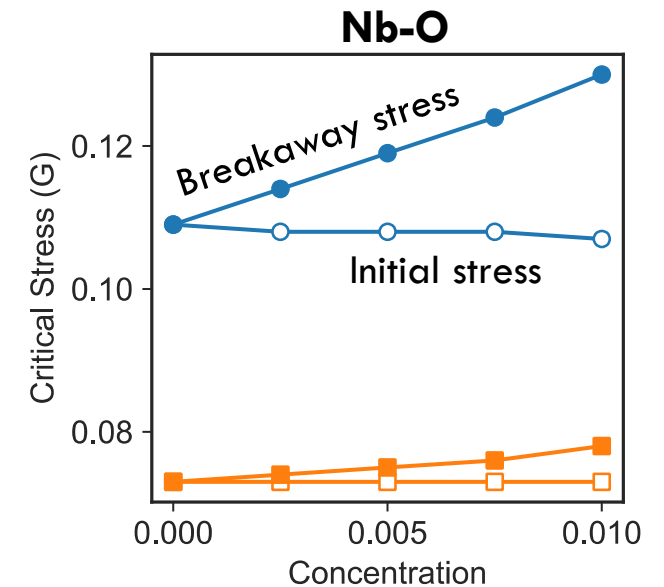
# Edge dislocation interstitial atmospheres

Initially homogeneous concentration  $c_0 = 0.01$



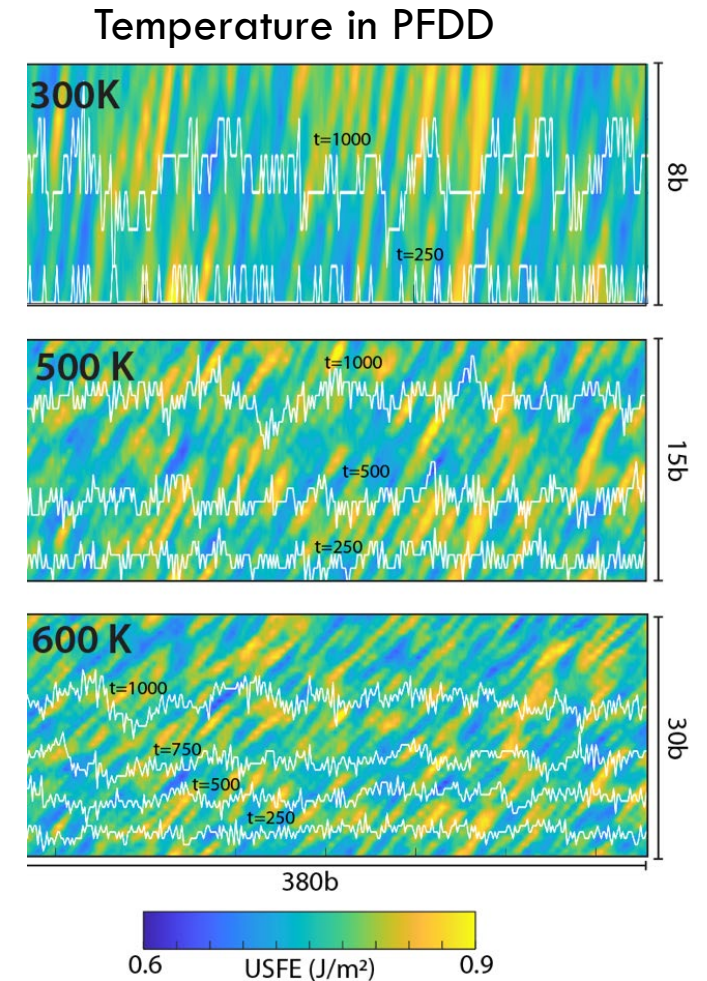
# Critical glide stresses

- Dislocations can glide a short distance before becoming pinned again (initial stress)
- Screw dislocation initial stress decreases with interstitial concentration for both Nb-O and W-H
- Breakaway stress for Nb-O increases with O concentration
- Breakaway stress for W-H is largely unaffected by concentration for both screw and edge



# Conclusions and Outlook

- Refractory MPEAs show promise as high-temperature materials
  - Dislocation mechanisms in MPEAs differ from pure refractory alloys
  - Dislocations controlled by athermal kink-pair nucleation
  - SRO increases critical dislocation stresses
- Interstitial-dislocation interactions must be understood for refractory alloys
  - O and H create different atmospheres due to their different site type occupation
  - H and O can alter dislocation behavior in opposite ways
- Future work
  - Include temperature in PFDD for thermally-activated mechanisms (kink-pair nucleation)



# Conclusions and Outlook

- Refractory MPEAs show promise as high-temperature materials
  - Dislocation mechanisms in MPEAs differ from pure refractory alloys
  - Dislocations controlled by athermal kink-pair nucleation
  - SRO increases critical dislocation
- Interstitial-dislocation interactions in alloys
  - O and H create different atmosphere type occupation
  - H and O can alter dislocation behavior in opposite ways
- Future work
  - Include temperature in PFDD for thermally-activated mechanisms (kink-pair nucleation)

Thank you!

